

## CHAPTER 7

# Development of advanced nanocomposite membranes by molecular sieving nanomaterials (zeolite and MOF)

Dayang Norafizan Awang Chee<sup>a,b</sup>, Mohamed Afizal Mohamed Amin<sup>a,c</sup>, Farhana Aziz<sup>a</sup>, Juhana Jaafar<sup>a</sup>, Ahmad Fauzi Ismail<sup>a</sup>

<sup>a</sup>Advanced Membrane Technology Research Centre (AMTEC), School of Chemical and Energy Engineering, Faculty of Engineering, Universiti Teknologi Malaysia, Johor Bahru, Malaysia

<sup>b</sup>Faculty of Resource Science and Technology, Universiti Malaysia Sarawak, Kota Samarahan, Malaysia.

<sup>c</sup>Faculty of Engineering, Universiti Malaysia Sarawak, Kota Samarahan, Malaysia

### 7.1 Zeolites

Zeolites are silicate or alumino-silicate crystalline materials formed by three-dimensional (3D) network of  $\text{SiO}_4$  and  $\text{AlO}_4$  tetrahedral configuration with open micropore size of 2 nm. Shared oxygen atoms link the 3D networks, creating linked cages or cavities. There are almost 100 different structural types of zeolite with different pore size, shape, and interconnectivity [1]. Some of the zeolites are shown in Fig. 7.1. The composition of the zeolite framework plays a vital role in determining the properties of the zeolites. The Si/Al ratio in synthetic zeolites varies considerably from 1:1 for zeolite X to near infinity in silicalite. These differences affect the hydrophilicity and acidity of the zeolites. Depending on their size, shape, and chemical characteristics, a combination of properties causes zeolites to interact very selectively with adsorbed molecules. Zeolites are known to exhibit microporous characteristics with uniform pore dimensions along with excellent ion exchange properties and ability to develop internal acidity, high thermal stability, and a high internal surface [2]. These features lead to their unique activity and selectivity, therefore making them suitable to be applied in liquid and gas separation.

#### 7.1.1 Preparation of zeolite membranes

According to Tavalaro et al. [2], the preparation of zeolite membranes can be done in four stages.

1. Pretreatment of the supports, involving thermal and plastic treatment, chemical treatment (preparation of anchoring layers) and mechanical treatment.

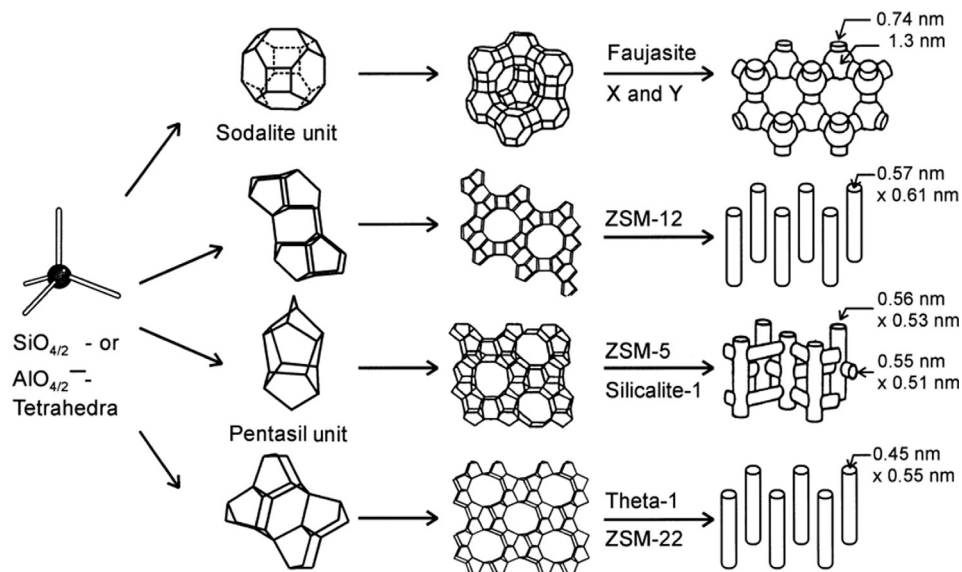


**Fig. 7.1** Structures of four selected zeolites (from top to bottom: faujasite or zeolites X, Y; zeolite ZSM-12; zeolite ZSM-5 or silicalite-1; zeolite Theta-1 or ZSM-22) and their micropore systems and dimensions. Adapted from J. Weitkamp, *Zeolites and catalysis, Solid State Ionics* 131 (2000) 175–188. DOI: 10.1002/9783527630295 with permission.

2. Synthetic methodology, which includes in situ synthesis on supports using gel or clear solution, seeding, etching, and microwave synthesis.
3. Impregnation on a stable or temporary support.
4. Elimination of small defects by chemical vapor deposition (CVD) method or selective coking.

In this chapter, the preparation of zeolite membranes is divided into self-supported membranes and membranes prepared with supports.

### 7.1.1.1 Zeolitic crystalline membranes: Self-supported membranes Self-supported zeolitic membranes prepared without supports

An ideal molecular sieving zeolitic membrane is a self-supported film made of thin, dense, and appropriately oriented zeolites [2]. A continuous and highly oriented membrane, with submicrometer thickness, requires a colloidal suspension nanometer-sized crystal precursor, followed by secondary growth of these particles to form a continuous film. Nanosols composed of packed zeolite particles with interzeolitic pores are used for membrane deposition. The pores can be closed through secondary growth (seeded growth procedure). Jung prepared TS-1 zeolite fiber films and monoliths using similar conditions [3], and it was found that the formation of fibers and films was affected by the high reactivity of the nanosized TS-1 zeolite and the crystalline content in aqueous solution.

On the other hand, Xu used a colloidal silica TPABr (tetrapropylammonium bromide) gel system under increased gravity to produce stronger films with better handling characteristics than membranes synthesized at normal gravity [4]. The high centrifugal force at increased gravity facilitates the intergrowth of the growing crystal. However, research also indicates that the increase in aluminum content will cause difficulty in producing good-quality zeolite films. Besides, a high-strength self-supporting NaA zeolite membrane was prepared from a geopolymer membrane through in situ hydrothermal transformation processing [5]. After the hydrothermal process, the surface and inner amorphous geopolymer membrane were converted into the zeolite crystal phase and the volume of the micropores of the hydrothermal sample changed from 0 to  $0.049 \text{ cc g}^{-1}$ . The membrane showed high compressive strength, approximately 57 MPa. Apart from that, a low-cost self-supporting membrane with high strength, good stability, and efficient separation capabilities was synthesized from faujasite zeolite through in situ hydrothermal synthesis [6]. This study indicated that extending hydrothermal treatment time enhanced the relative crystallinity and surface density of the zeolite membrane. As the membrane showed good performance in separating alcohol/water system with low-cost materials, it can be used as a substitute for traditional zeolite membranes for large-scale industrial demand.

### **Self-supported zeolitic membranes prepared on temporary supports**

After the crystallization process, zeolitic films can be synthesized and detached from their substrate (temporary support) to form self-supported films. Sano et al. have synthesized self-supported ZSM-5 zeolite films on Teflon sleeves [7]. The outer and inner side of the film showed significant differences, with the outer side of the film showing the aggregation of crystals, while no clear shape of zeolite crystals was observed in the inner side of the film. Sano et al. also synthesized highly siliceous zeolite films of silicalite and ZSM-5 by using cellulose molding [8]. The study revealed that the zeolite synthesis using filter paper needed a longer crystallization period compared to the Teflon slab. However, zeolite films prepared using cellulose molding were found to be highly siliceous with high structural strength; the shape of zeolite film can be controlled easily. Anderson and his co-workers prepared a self-supported membrane using polymeric material as temporary supports [9]. Self-supporting polycrystalline films of zeolites ZSM-5 and gmelinite, one crystal thick, have been synthesized on polytetrafluoroethylene (PTFE) and polysulfonated styrene substrates. ZSM-5 film was synthesized using tetrapropylammonium bromide or hexadamine as templates, whereas gmelinite film was synthesized using Dab-4-Br polymer as a template. The prepared films exhibited high crystallinity and high adsorption capacities and demonstrated the potential for growing molecular-sieve membranes. The polymer, made of 1,4-diazobicyclo (2.2.2) octane (DABCO) and 1,4-dibromobutane, seems to have a strong anchoring effect on the zeolite during membrane synthesis. Yamazaki also used PTFE as a temporary support to produce a

modernite membrane with prismatic crystals of  $30 \pm 50$  nm in length formed at the hydrogel side and rectangular prisms on the plate side [10]. The membrane could be easily peeled off from the substrate without any damage. The Si:Al ratio of the membrane was independent of the crystallization period and was about 6.5 and 7.5 for the hydrogel and plate sides, respectively. Another type of self-supported zeolite membrane known as hydroxysodalite (HS) was synthesized successfully by hydrothermal method using natural kaolin [11]. In this research, the synthesis of an HS zeolite membrane from an extruded tube of kaolin was investigated. Firstly, kaolin was calcined at  $500\text{--}850^\circ\text{C}$  to the meta-kaolinite phase, and then the zeolitization experiments were carried out under hydrothermal conditions. The resultant metakaolinite was reacted with NaOH solutions in autoclaves at  $100^\circ\text{C}$ . The X-ray diffraction (XRD) patterns of the membranes exhibited peaks corresponding to the zeolite.

#### **7.1.1.2 Zeolite composite membranes: Zeolitic membranes on stable supports Zeolite membranes on metallic supports**

Self-supported zeolitic membranes are known to have fragile and unstable characteristics, making them unsuitable for most applications. Therefore, most researchers prefer to use supported membranes for their studies. Synthesis mixture containing silica, tetrapropylammonium, and water was used to form continuous silicalite-1 layer supported on porous sintered stainless steel at 353 K by using hydrothermal method [12]. The overall porosity of the support was 0.52 while the top layer had a porosity of over 0.6 and an average pore size of about 50  $\mu\text{m}$ . The average pore size of the coarse part was about 200  $\mu\text{m}$ . The SEM images revealed that the membrane consists of a relatively large layer of intergrown silicalite-1 crystals on top of the porous stainless-steel support. However, there were randomly oriented crystals, which were not well interconnected, that grew on top of the intergrown layer. Therefore, the real membrane thickness may be less than the observed 50–60  $\mu\text{m}$ .

Another type of metallic supported membrane known as A-type zeolite membranes were prepared on nonporous stainless steel ( $55 \times 35 \times 1.5$  mm) by using the electrophoretic method [13]. To prepare the membrane, the support surface was first polished with 700 grit-sand paper, then cleaned with deionized water in an ultrasonic cleaner before being immersed in  $0.1 \text{ mol L}^{-1}$  hydrochloric acid solution for 4 h. The support layer was again cleaned with deionized water before proceeding to the electrophoretic synthesis method. Then, two metal supports were placed vertically on a Teflon holder and then were placed vertically in stainless steel autoclave. The synthesis solution was poured into the autoclave, and then the autoclave was sealed with a rubber plug. A DC power supply used was varied from 0 to 2.0 V. After crystallizing for 1–12 h at 363 K, the solution was removed, and the membrane was washed with the deionized water, and then dried. The results showed that the negatively charged zeolite particles were able to migrate to the anode metal surface evenly and rapidly under the action of the applied electric field,

consequently formed a uniform and dense membrane in a short time. The results also indicated that applied potential had a significant effect on membrane formation. Zeolite membranes prepared with 1 V potential produced more uniform and denser zeolite membranes compared to the other applied potential.

Zhang reported the preparation and separation testing of a NaA (or 4A-type) water-selective zeolite membrane supported on a robust, porous Ni sheet 50  $\mu\text{m}$  thick [14]. The substrate of membrane (Ni) was coated with NaA seeding crystals of 0.3  $\mu\text{m}$  prior to the slip-coating process being performed to obtain good coverage of NaA seeds on the substrate. Then, the hydrothermal synthesis was continued to obtain the NaA membrane. Metal-supported clinoptilolite membranes were also prepared by Farjoo et al. to study the hydrogen permeation of the membrane [15]. The membrane preparation involved the coating of the pretreated stainless-steel tubes with clinoptilolite powder, 50 wt% aluminosilicate binder, and 25 wt% distilled water. Coated tubes were air-dried at room temperature and pressure before being sintered at 371°C at 2°C min<sup>-1</sup> for 4 h. The coated tubes were also subjected to a second coating. The resulting single- and double-layered membranes were 50 and 80  $\mu\text{m}$  thick, respectively.

### Zeolite membranes on ceramic supports

A ceramic-supported zeolite membrane is another option to produce better stability of zeolite membrane. Basumatary et al. prepared three types of zeolite membrane, MCM-41, MCM-48, and FAU, on a low-cost, circular ceramic support by hydrothermal treatment [16]. The sintered ceramic supports were polished with abrasive paper (no. C-220) and were cleaned before being subjected to zeolite synthesis gel in a Teflon autoclave reactor for hydrothermal reaction. After treatment, the membranes were washed and sintered.

Further, an NaY zeolite membrane was prepared on an alumina disk by a secondary method (rubbing), and the influence of the ceramic supports investigated [17]. The NaY zeolite membrane was prepared using the secondary growth (rubbing) technique as shown in Fig. 7.2. The crystals deposited on the ceramic support ( $\alpha$ -alumina or  $\gamma$ -alumina) were then carefully rubbed manually, then was fixed with a Teflon holder in a 70-mL Teflon-coated autoclave. The synthesis gel containing precursors of NaY zeolite (60 mL) was then placed in the autoclave at 90°C for 7 h duration.

The SEM image showed that the  $\alpha$ -alumina or  $\gamma$ -alumina is completely covered with Y zeolite crystals. The membrane exhibited hydrophilic characteristics and demonstrated excellent performance for oil rejection, both for NaY/ $\alpha$ -alumina and NaY/ $\gamma$ -alumina.

Xu and coworkers synthesized Zeolite X membranes by in situ hydrothermal synthesis method on porous  $\alpha$ -Al<sub>2</sub>O<sub>3</sub> ceramic tubes [18]. The ceramic tubes with a pore size of 50–200 nm were precoated with zeolite X seeds or precursor amorphous aluminosilicate. The zeolite X crystals were synthesized by the classic method and mixed into deionized water as a slurry with concentration of 0.2–0.5 wt%. Zeolite seed was deposited into



**Fig. 7.2** Zeolite membranes preparation by secondary growth method (rubbing). Adapted with permission from A. dos S. Barbosa, A. dos S. Barbosa, T.L.A. Barbosa, M.G.F. Rodrigues, *Synthesis of zeolite membrane (NaY/alumina): effect of precursor of ceramic support and its application in the process of oil–water separation*, *Sep. Purif. Technol.* 200 (2018) 141–154. DOI: 10.1016/j.seppur.2018.02.001.

pores near the inner surface of alumina tubes and crystallization was allowed for 24–96 h, at 95°C. The thickness of top layers reported was 10–25  $\mu\text{m}$  and zeolite crystals can penetrate into pores of the supports as deeply as 100  $\mu\text{m}$ . From this study, precoating of zeolite seeds on supports was proven to shorten the synthesis time and improve the membrane strength.

Surface modification on a ceramic substrate is one of the best means to achieve a uniform layer of zeolite membrane on the ceramic. Silicalite-1 zeolite film (membrane) was grown hydrothermally via secondary crystallization on porous alumina discs through its surface modification with 3-aminopropyl triethoxysilane (APTES) [19]. The same silicalite-1 membrane was prepared on the unmodified support surface via secondary crystallization for comparison purpose. A schematic for the formation of a silicalite-1 membrane (film) on a porous ceramic substrate through surface modification technique is shown in Fig. 7.3.

Compared to that crystallized (ex situ) on an unmodified support surface, a better interlocking of the silicalite-1 crystals was obtained in the film after the secondary crystallization (ex situ) of the seed-coated support modified with APTES as shown in Fig. 7.4.

Recently, a new method for synthesizing ZSM-5/NaA hybrid zeolite membrane on 170-mm-length ceramic tubes was reported [20]. The new method employed kaolin as the modified layer in the process of hydrothermal synthesis. Firstly, kaolin was filtrated on the surface of the support as the modified layer. The kaolin layer served as the interface interlinkage among support, NaA membrane, and ZSM-5 membrane layers, apart from promoting the growth of zeolite membranes. Therefore, more compact and



homogeneous NaA and ZSM-5 zeolite layers were formed. The permeation separation experiments also demonstrated that the performance of ZSM-5/NaA hybrid membrane was better than that of the monolayer zeolite membrane with the permselectivities of H<sub>2</sub> over CO<sub>2</sub>, N<sub>2</sub>, CO, and CH<sub>4</sub> being 5.40, 4.65, 4.70, and 3.93, respectively, being higher than the corresponding Knudsen diffusion coefficients.

### **7.1.1.3 Zeolite-filled polymeric membranes**

Another method to obtain a good zeolitic membrane is to bind together the polymeric materials with the zeolite crystals. Evcin and Tutkun prepared zeolite-filled polymeric membrane using two types of zeolites, namely, zeolite 3A (hydrophilic type) and silicalite-1 (hydrophobic type) [21]. The zeolites were activated by heat treatment to remove the residual contaminant. Silicalite-1 was activated at 600°C and zeolite 3A at 400°C for 6 and 4 h, respectively, and kept in a desiccator at room temperature. Zeolite-filled PDMS membranes were obtained from 60% isooctane solution of precursors and various quantities of desired zeolites. The homogeneous mixtures were placed on a clean and smooth glass plate using a doctor's blade, and the casting solution was allowed to be evaporated at 70°C in an oven for 12 h and cooled to room temperature. The obtained elastomer material was immersed in a water-ethanol for the phase-inversion process. The zeolite-filled PDMS membranes were tested for their performance for pervaporation.

Duval et al. prepared zeolite-filled glassy polymeric membrane for gas separation properties [22]. However, the main problem of this study is to ensure that the zeolite particles are properly attached to the glassy polymers. Therefore, to overcome this problem, Duval and his coworkers modified the surface of zeolite particles with a silane agent. The modified zeolites showed good attachment with the PEI polymer as it showed improvement of the internal structure of silicalite-filled PEI membranes. Duval also explained that the proper attachment might be due to the amino functional silanes, which efficiently improve the adhesion of thermosetting, and thermoplastic resins to mineral surfaces. The mechanism often assumed or postulated is the formation of an interpenetrating polymer network (IPN) at the mineral surface when no reaction between the amino group of the coupling agent and the polymer chain is possible. The improvement observed in this study might be due to the formation of an IPN with the silane coupling agent; the polymer chains remain in contact with the mineral surface upon evaporation of the solvent. The gas permeation results, however, could not illustrate this improvement.

Novel polymeric membranes were prepared by incorporating the 13 × zeolite into chitosan (CS) by solution casting [23]. The preparation involved the incorporation of zeolite into the chitosan membrane with the presence of glutaraldehyde as a crosslinker. In this study, the amount of chitosan was kept constant, whereas the amount of 13 × zeolite was varied. The chitosan membrane showed preferential permeation to water for 5%–40% water-in-feed compositions. The experimental results further

revealed that both the flux and selectivity increased simultaneously with increasing zeolite content in the membrane. The presence of zeolites in the membrane matrix proved to be able to increase the hydrophilicity, selective adsorption, and molecular sieving action of the membrane. These might be due to the creation of pores by the zeolites in the membrane matrix. The membrane containing 30 wt% of zeolite shows the highest separation selectivity of 1620 at 30°C for 5 mass% of water in the feed.

## 7.1.2 Application of zeolites membranes for separation

### 7.1.2.1 Gas separations

The good attributes of zeolite membranes might benefit several important industrial processes such as air separation ( $N_2/O_2$ ) [24], the recovery of hydrogen from gas mixtures ( $H_2/N_2$ ,  $H_2/CO$ ,  $H_2/CO_2$ ,  $H_2$ /hydrocarbons) [25], hydrocarbon separation (olefins/paraffins, linear/branched isomers) [26], and  $CO_2$  capture from natural gas [27]. However, there are no documented commercial examples of zeolitic membrane applications in gas separations, perhaps due to the relative difficulty of producing defect-free zeolitic membrane fabrication as well as the lack of novel design of cost-effective, high area packing density zeolitic membrane modules to compete with commercial spiral-wound or hollow-fiber polymeric gas separation membrane modules [28]. Therefore, more and more research has been conducted to fulfill the demand from industry, particularly to produce a good-quality commercial membrane with inexpensive material.

The  $CO_2$  separation over  $CH_4$  in the zeolite is due to the favorable adsorption of  $CO_2$  over  $CH_4$ . For most zeolites, for example, faujasite (FAU) and MFI types, the separation performance normally decreases with increasing temperature as well as the molecular sieving mechanism due to their different molecular kinetic diameters with  $CO_2$  of 3.30 Å and  $CH_4$  of 3.80 Å [29,30]. The selectivity of  $CO_2/CH_4$  is quite dependent on the zeolite material composition. ZSM-5, with larger pores of 5.5 Å, displayed a lower selectivity, around 5 at room temperature [31]. Comparably, more promising membranes are made from SAPO-34 or DDR-type zeolites, having pores of 3.8 and 3.6 Å, respectively. SAPO-34 zeolite membrane on porous alumina supports exhibited a  $CO_2/CH_4$  selectivity range from 86 to 171, with  $CO_2$  permeabilities of 20,000–40,000 Barrer [32].

Significantly improved zeolite membranes for  $N_2/CH_4$  separation were prepared by using high-aspect-ratio zeolite seeds. Semicircular seeds with a high aspect ratio (AR) facilitated the growth of thinner continuous SAPO-34 membranes of much higher quality [33]. These membranes showed  $N_2$  permeances as high as  $(2.87 \pm 0.15) \times 10^{-7} \text{ mol m}^{-2} \text{ s}^{-1} \text{ Pa}^{-1}$  at 22°C with  $N_2/CH_4$  selectivity (9–11.2 for equimolar mixture). These thinner SAPO-34 membranes were able to increase the  $N_2$  permeance by 1.4 times, with the addition of more silicon, without sacrificing the  $N_2/CH_4$  separation. Another type of zeolite membrane was prepared from SAPO-34 by secondary growth in the absence of organic templates via hydrothermal treatment with microwave heating [34]. In this study, the researchers were able to produce a continuous

SAPO-34 molecular sieve membrane with the avoidance of organic templates, the calcination defects, and environmental pollution. The membrane also displayed extremely high CO<sub>2</sub>-CH<sub>4</sub> separation performance. Nevertheless, continuous and high silica SSZ-13 zeolite membranes were prepared on porous mullite supports from high SiO<sub>2</sub>/Al<sub>2</sub>O<sub>3</sub> ratio or aluminum-free precursor synthesis gel [35]. From the research, it was found that single gas permeance (CO<sub>2</sub> and CH<sub>4</sub>) of the high silica SSZ-13 zeolite membrane decreased with the SiO<sub>2</sub>/Al<sub>2</sub>O<sub>3</sub> ratio in the precursor synthesis gel, while the ideal CO<sub>2</sub>/CH<sub>4</sub> selectivity of the membrane was gradually increased.

Another study was conducted to produce good separation performance of DDR3 zeolite membrane for separation of CO<sub>2</sub> and N<sub>2</sub> from CH<sub>4</sub> [36]. The study compared two synthesis methods on the performance of the membrane to separate CO<sub>2</sub> and N<sub>2</sub> from CH<sub>4</sub>. The synthesis of DD3R zeolite membrane with low SiO<sub>2</sub>/H<sub>2</sub>O ratio ( $\leq 0.01$ ) is a better method to create a DD3R zeolite layer with good quality on the surface of alumina support. The low SiO<sub>2</sub>/H<sub>2</sub>O ratio led to better coverage of the support surface by a dense zeolite layer and performed well for the separation of CO<sub>2</sub> and N<sub>2</sub> from CH<sub>4</sub>.

### 7.1.2.2 Liquid separations Pervaporation

Pervaporation is considered one of the most promising technologies for liquid separations in the biorefinery, petrochemical, and pharmaceutical industries, especially for some liquid mixtures that are not suitable for filtration [37]. When a liquid mixture is in contact with one side of the membrane, the membrane absorbs components. The adsorbents diffuse through the membrane and evaporate as permeates on the other side of the membrane, induced by a vacuum or gas purge. The difference in sorption and diffusion leads to the separation of components. A type of zeolite membrane, which has been applied in large-scale production, is a zeolite NaA layer (LTA structure type) on a tubular alumina support. Other types of membranes are at the stage of laboratory research or pilot tests. Zeolite NaA membranes are used in pervaporation processes to remove water from mixtures of organic/water. Usually, high-cost operations are used, such as variable pressure distillation and extractive or azeotropic distillation. The use of membrane technologies can reduce resource and energy consumption. NaA membrane showed high efficiency due to the optimum pore size for the filtration of water molecules (0.296 nm) and its hydrophilic properties [38]. The first partly commercial introduction of zeolite membranes was performed by the Mitsui Engineering & Shipbuilding Corp. (Japan) in 1999 using a plant with a membrane area of 60 m<sup>2</sup> [39]. The plant is used to dehydrate organic liquids, primarily ethanol, via pervaporation or separation of vapors and the capacity of the plant was 50 L h<sup>-1</sup>. Tubular membranes with a length of 80 cm were assembled into modules; each of these modules contained 125 components. Apart from Mitsui Company, other companies such as Nano-Research Institute Inc. (XNRI), a

100% subsidiary of Mitsui & Co., and the European alliance between Smart (United Kingdom) and Inocermic (Germany) produced a hydrophilic LTA zeolite layer on ceramic tubular support [40]. The membrane showed a good selectivity in the separation of water from organic solutions by steam permeation and pervaporation. XNRI has installed vapor permeation units in Brazil ( $3000 \text{ L day}^{-1}$ ) and India ( $30,000 \text{ L day}^{-1}$ ) at an operation temperature of  $130^\circ\text{C}$  for the water removal of bioethanol using LTA membranes.

Then, XNRI developed a high flux faujasite membrane of types X and Y on  $\alpha$ -alumina support, a more chemically stable membrane compared to LTA membranes. For test mixtures of water (10 mass%) and ethanol (90 mass%) at  $75^\circ\text{C}$  the X-type achieved fluxes of  $6\text{--}9 \text{ kg m}^{-2} \text{ h}^{-1}$ , with a separation factor of 100–400 whereas the Y-type able to achieve fluxes of  $4 \text{ kg m}^{-2} \text{ h}^{-1}$ , with a separation factor of about 150. The collaboration between Smart Chemicals Development and Inocermic GmbH supported membranes of type LTA are produced in a half-industrial scale in Germany (see Fig. 7.5).

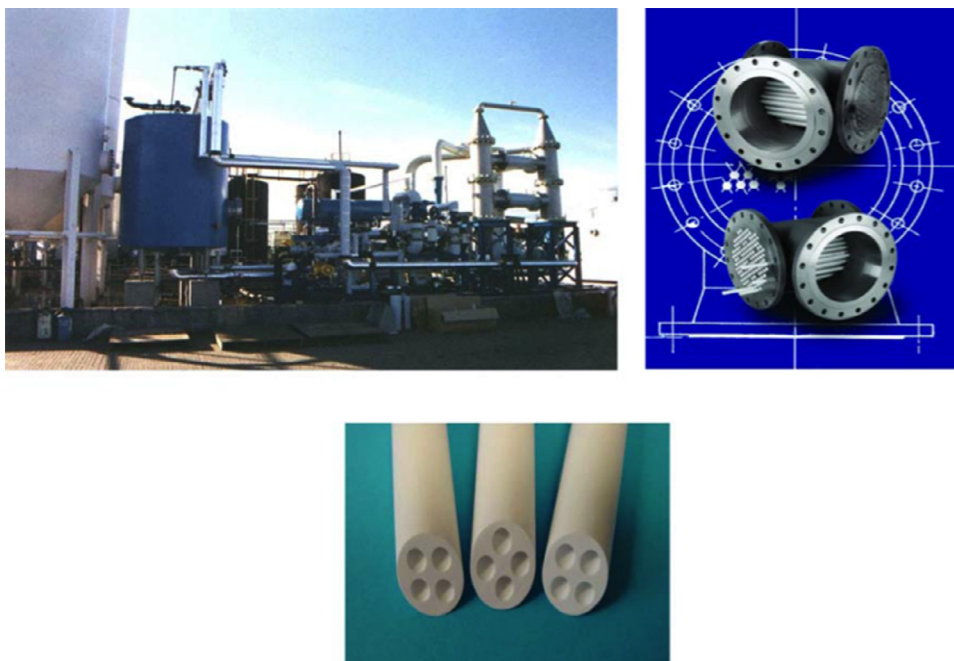


**Fig. 7.5** Semitechnical pervaporation plant for the dehydration of ethanol in the United Kingdom. The modules of  $5.8 \text{ m}^2$  membrane area each are equipped with 4-channel Smart zeolite membranes produced by the Inocermic GmbH, Germany. Adapted with permission from J. Caro, M. Noack, P. Kolsch, Zeolite membranes: from the laboratory scale to technical applications, *Adsorption* 44 (2005) 215–227.

## Water treatment

Zeolite membranes have been extensively studied for more than 15 years. Most of the research has focused on the potential for zeolite membranes in gas separation and pervaporation processes. However, a few years ago, molecular dynamic simulation proved theoretically that zeolite membranes are able to remove ions from aqueous solution through reverse osmosis. Hydroxysodalite (HS) zeolite membrane prepared through a hydrothermal method on porous tubular mullite support (14-mm outer diameter, 10-mm inner diameter, and 10-cm length) showed promising RO performance for concentrated solutions containing different types of cations [41].

Zeolite membranes are also used in the treatment of wastewater and desalination process due to their promising characteristic regarding thermal and chemical stability for liquid separation. An MFI-type zeolite membrane was developed on a tubular  $\alpha$ -alumina substrate by a combined rubbing and secondary hydrothermal growth method [42]. When saline wastewater was fed at 7 MPa to the zeolite membrane, it showed a salt rejection of 80% based on electrical conductivity (EC) and a flux of  $4 \text{ L m}^{-2} \text{ h}^{-1}$ . When the operating pressure was set at 3 MPa, slightly lower salt removal was observed. The EC of feed water showed the increment over 48 h test time, indicating the 43% water recovery, yet the EC reduction remained  $>70\%$ , and the flux remained at around  $2 \text{ L m}^{-2} \text{ h}^{-1}$  throughout the test period. This indicated that the membrane was resistant to organic fouling and the chlorine stability studies also confirming the chemical stability of the zeolite membranes.

The incorporation of zeolites nanoparticles into TFC RO membrane is also known to improve the water permeability of the membrane. However, some of the zeolites, for instance, NaA, might limit the application of the TFN for seawater desalination. Therefore, the chemically stable silicalite-1 nanoseolite was incorporated into the skin layer of the RO composite membrane via interfacial polymerization technique [43]. The membrane exhibited excellent chemical stability toward acid and multivalent cation, compared with the NaA-mixed membrane. Besides, silicalite-1 showed a better permeability than NaA, due to larger channel pores and a higher water diffusion rate in silicalite-1. Therefore, silicalite-1 mixed membrane has great potential in large-scale seawater desalination. A study to separate trivalent salts ( $\text{FeCl}_3$  and  $\text{AlCl}_3$ ) from aqueous solution using Faujasite (FAU) zeolite composite ultrafiltration on ceramic support prepared by facile uniaxial support showed a maximum rejection of 81% for  $\text{FeCl}_3$  and 75% for  $\text{AlCl}_3$  at an applied pressure of 276 kPa for feed concentration of 250 ppm [44].

Yurekli incorporated the NaX nanoparticles in PSf membrane to remove lead and nickel cations from synthetically prepared solutions [45]. The performance of the hybrid membrane was determined under dynamic conditions. From this study, the sorption capacity and water hydraulic permeability of the membrane can be improved by tuning the fabrication condition, for example, the evaporation period of the casted film and the NaX loading. The maximum sorption capacity of the hybrid membrane for the lead and nickel ions was measured as 682 and  $122 \text{ mg g}^{-1}$ , respectively (60 min of filtration, 1 bar of transmembrane pressure). The coupling process suggested that membrane architecture

could be efficiently used for treating metal solutions with low concentrations and trans-membrane pressures.

## 7.2 Metal-organic framework (MOF)

Metal-organic frameworks (MOFs) are a new class of porous hybrid organic/inorganic materials, with zeolite-like features. MOFs are known to be stable up to temperatures above 200°C, and are characterized by very high surface areas, due to the porosity of the structures [46]. The MOF structures consist of metallic clusters and organic linkers; these combinations give many possible arrangements between metals and organic compounds to form particles with different textural, chemical properties, porosity, and flexibilities [47]. The nodes of the MOF structure are formed from metal ions, or metal ion clusters called secondary building units (SBUs), and organic ligands bridge the SBUs in regular, geometric patterns [48]. The wide diversity of SBUs and connectivity of the ligands allows for a variety of networks. For instance, a combination of  $Zn^{2+}$  with 1,4-benzene dicarboxylic acid ( $H_2bdc$ ) yields IRMOF-1. When the same metal is combined with different ligand (2-methylimidazole), ZIF-8 will form. The different MOFs structures are shown in Fig. 7.6.

### 7.2.1 Preparation of MOFs membranes

#### 7.2.1.1 *In situ* preparation

##### Growth on unmodified support

The synthesis of ZIF-8 through in situ growth involves only one step; immersing the support in the growth solution without any preattached crystal on the surface of the

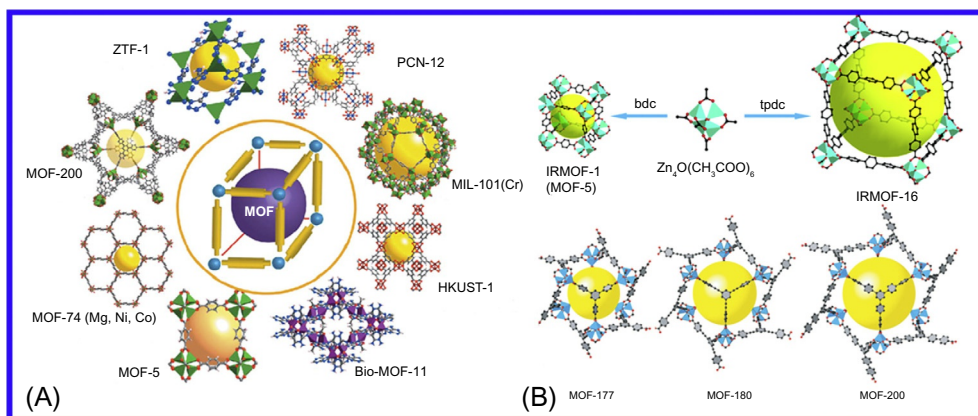


**Fig. 7.6** MOF structures with different metal and organic linkers. (A) represents the important MOFs reported for high gas storage properties, (B) ditopic carboxylate linkers with different lengths to produce a variety of MOFs materials with the same network topology. Adapted with permission from Y. Zhao, Z. Song, X. Li, Q. Sun, N. Cheng, S. Lawes, *Metal organic frameworks for energy storage and conversion*, *Energy Storage Mater.* 2 (2016) 35–62. doi:10.1016/j.ensm.2015.11.005.

support. All the nucleation, growth, and intergrowth of crystals on the substrate occur during the same fabrication step [49]. However, Shah et al. [49] noted that the absence of strong interfacial bonding is a common challenge in the fabrication of MOF on the native substrate. This might be affected by the surface chemistry of the support, for example, the zeta potential and surface acidity [50]. Xu et al. [51] reported on the in situ growth of ZIF-8 on alumina hollow fiber membrane outer layer from a concentrated synthesis gel with a molar composition of 1  $\text{Zn}^{2+}$ : 8 Hmim: 75 methanol. The alumina hollow fiber membrane was heated at 80°C overnight before being placed in Teflon-lined autoclave. The ZIF-8 synthesis solution was poured into the autoclave, and heating at a given temperature (25°C, 100°C, and 150°C) for 5 h. The ZIF layer is well grown on ceramic substrate, and its thickness is about 6  $\mu\text{m}$  with some ZIF-8 crystals is likely to present in the pores of alumina support. The FIB-SEM image of the cross-section of ZIF-8 layer reveals that ZIF-8 layer also possesses many irregular-shaped microcavities.

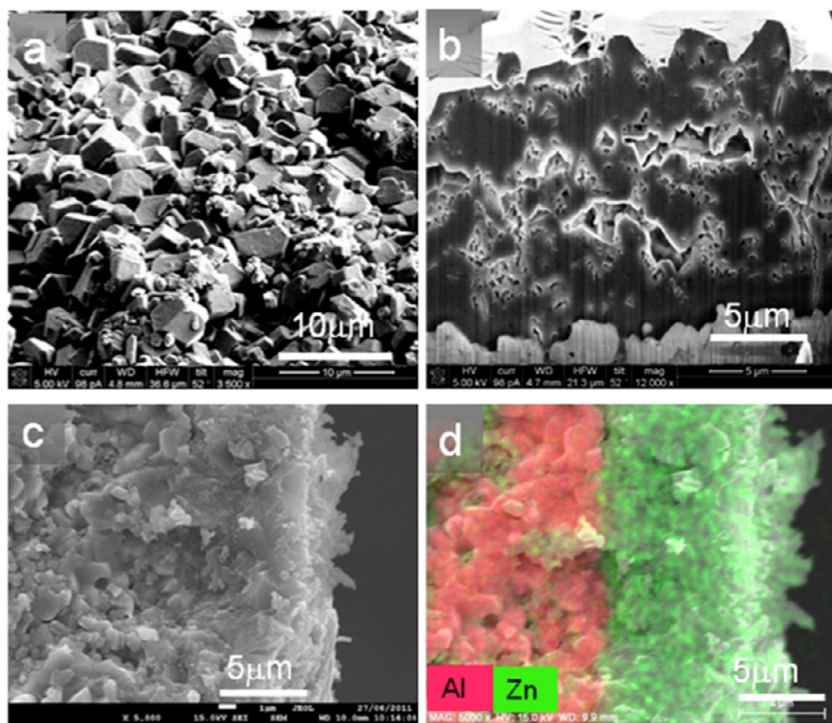


**Fig. 7.7** SEM images of ZIF-8 membranes supported on the ceramic hollow fiber prepared from the high-concentration synthesis gel at 100°C for 5 h: (A) surface, (B) cross-section created by FIB, (C) cross-section, and (D) elemental mapping image of the cross-section. Adapted with permission from G. Xu, J. Yao, K. Wang, L. He, P.A. Webley, C. sheng Chen, H. Wang, Preparation of ZIF-8 membranes supported on ceramic hollow fibers from a concentrated synthesis gel, *J. Membr. Sci.* 385–386 (2011) 187–193. doi:10.1016/j.memsci.2011.09.040.

Fig. 7.7 shows the SEM image of the prepared membrane. Apart from that, in situ growth of ZIF-8 using interfacial synthesis approach was reported by Li et al. [52]. In this approach, ZIF-8 membranes were synthesized on porous polyethersulfone supports based on a liquid-liquid interfacial coordination mechanism by firstly, saturating the substrate with the aqueous zinc nitrate, followed by pouring an octanol-based 2-methylimidazole solution on the surface. After a certain reaction time, a selective ZIF-8 layer was formed on the porous polymeric support. According to the cross-section images, the ZIF-8 layer only has a thickness of around 250–300 nm.

### Growth on modified support

As mentioned in the previous section, the ZIF-8 membrane on unmodified supports is prone to several problems, such as cracking. Therefore, a further modification of the support surface is sometimes crucial to develop a crack-free ZIF-8 membrane. McCarthy et al. [53] reported the synthesis of ZIF-8 membranes by modifying the support with ligand 2-methylimidazole solution through a thermal deposition method. The ligands bonded to the surface of the support through an activation process, forming a strong aluminum-nitrogen covalent bond at 200°C. The researchers also mentioned that the presence of sodium formate is also important to obtain continuous and thoroughly intergrown ZIF-8 membranes because the high pH value sparked the deprotonation of surface linkers, enhancing the quality of the membrane formed.

For the poorly intergrown membrane, a secondary growth method was applied using the membrane as seeded support and regrown into a well-intergrown membrane in the presence of sodium formate. The researchers also found zinc chloride to be a better zinc source compared to zinc nitrate in forming a well-intergrown ZIF-8 membrane. However, no film was obtained after a synthesis time of 36 h using zinc chloride without the presence of sodium formate.

In 2013, Zhang et al. reported on a scalable and straightforward method for preparing low-defect ZIF-8 tubular membranes, by modifying the substrate surface with an ultrathin ZnO layer, followed by surface activation with Hmim solution [54]. The ZnO and Hmim reacted, creating uniform nucleation sites on the surface of the ZnO layer. This is thought to be responsible for the good performance of the membrane in terms of its permeability and permselectivity. Moreover, the resulting excellent adhesion between the ZIF-8 and ZnO also prevented delamination.

Wang et al. [55] reported on the in situ growth of ZIF-8 on porous alumina and zinc oxide hollow fiber membrane, with only 5–6 μm thickness with a crack-free ZIF membrane, which exhibits excellent hydrogen separation performance. The surface functionalization with Hmim is one of the vital aspects for successful ZIF growth. It is believed that the Hmim could react with ZnO to form a series of Hmim coordinated Zn<sup>2+</sup> compounds, which are important precursors to promote the embryonic ZIF-8 nuclei.

### 7.2.1.2 Secondary (seeded) growth

In comparison with the in situ growth method, the secondary or seeded growth method involved the seeding of nuclei onto the support where the membrane would subsequently grow [56]. Algieri et al. also stated that their method is favorable due to the thinner and less defective membrane produced because each step involved can be independently manipulated. However, this method is relatively complex compared to the in situ growth method explained earlier. The seeding method can be done through various techniques, for instance, dip-coating [57,58], rubbing [59], reactive seeding [60], and immersion [61].

In 2012, Pan et al. synthesized the ZIF-8 membrane by dip-coating using a seeded hydrothermal growth on yttria-stabilized zirconia (YSZ) fiber support [58]. In the method, YSZ support was dipped in the seed suspension for 10 s, producing a  $\sim 2.5$   $\mu\text{m}$  membrane. However, the overall coverage of the ZIF-8 particles was relatively low due to the blockage of the seeds inside the pores of the YSZ. Venna and Carreon [62] also reported on the synthesis of ZIF-8 membrane using secondary seeded growth but with rubbing method and in situ crystallization. The seeding process was prepared using hydrothermal method, and the support was calcinated under  $900^\circ\text{C}$  for 30 min prior the rubbing process with dry ZIF-8 seed. The membrane was 5–9  $\mu\text{m}$  thick.

In 2016, Lai and his coworkers reported a preliminary study on the preparation of ZIF-8 membrane on  $\alpha$ -alumina via in situ growth, as well as secondary growth using the rubbing and dip-coating methods [63]. From SEM images in the preliminary study, the researchers found uncovered porous support areas and the ZIF-8 grains formed on the support are not uniform. For the ZIF-8 membrane synthesized through the rubbing method, the crystal size was in the range of 1–4.7  $\mu\text{m}$ , whereas the dip-coating method produced crystals with a size of 2.5–5  $\mu\text{m}$ . These results imply that secondary growth can result in a poorly intergrown ZIF-8 layer if the seed layer is not formed properly. On the other hand, the in situ growth of ZIF-8 on the support membrane showed better formation. The continuous, small, and loosely packed ZIF-8 grains observed at 4 h synthesis time, and better coverage of ZIF-8 on alumina can be seen through SEM image. However, defects were observed when the synthesis time increased to 36 h. Nevertheless, in terms of size, the ZIF-8 grains obtained at 36 h are relatively uniform, ranging from 1.5 to 2.2  $\mu\text{m}$ .

Some researchers reported the use of sodium formate to further improve the ZIF-8 deposition on the support. For example, McCarthy et al. reported the effect of sodium formate in the heterogeneous nucleation and growth of ZIF crystals [53]. Shah et al. [64] also reported specifically on the role of sodium formate for producing well-intergrown continuous ZIF-8 membranes on unmodified support. It was found that the existence of sodium formate can enhance the heterogeneous nucleation of ZIF-8 crystals on alumina supports, besides being able to promote intergrowth of ZIF-8 crystals. It was confirmed that sodium formate reacts with zinc source to form zinc oxide layers on  $\alpha$ -alumina supports, which in turn promote heterogeneous nucleation.

### **7.2.1.3 Microwave-assisted growth of ZIF membranes**

The remarkable advantages of microwave technology for chemical synthesis have provoked growing interest among researchers. Microwave technology may help to reduce synthesis time. It is claimed as green technology because it does not produce any hazardous material like gas fumes. Nor is it heated using an external energy source [65]. Kwon and coworkers [66] reported a rapid and simple microwave-assisted seeding technique for the synthesis of high-quality ZIF-8 membrane. The microwave seeding process involves three steps: first, saturating the porous support with a metal solution, then exposing the saturated support to ligand precursor, and lastly by rapid crystal formation under microwave irradiation. It is crucial to maintain a high concentration of both precursors on the support prior to microwave irradiation because it will maximize the heterogeneous crystal formation and at the same time, minimize the undesirable homogeneous crystal formation. Additionally, the rapid absorption of microwave energy by metal ions inside the supports further increases the local temperature inside the support, resulting in the rapid formation of ZIF-8 inside and on the surface of the supports.

Recently, a study on the preparation of mixed metal, CoZnZIF-8, with various Co/Zn contents and mixed ligand ZIF-7-8 using microwave irradiation method was reported [67]. This study is the first example of a one-step synthesis of mixed metal, and ligand CoZn-ZIF-7-8 successfully obtained using microwave irradiation. Other than the short synthesis time, crystallization using microwave irradiation produced higher yield, reduced the amount of ligand and solvent, and eliminated the use of deprotonators when compared to conventional methods reported earlier.

### **7.2.1.4 Blending method**

Another approach to fabricate MOF membranes is a blending method to produce MOF-based MMMs. The blending method is more reproducible and requires no expensive supports. The membrane produced is more stable rather than bare MOF, especially long term, compared to the membrane prepared by the previously explained method. Two methods, substrate-based blending, and substrate-free blending, were developed to design MOF-based MMMs for liquid separation [68]. Substrate-based blending was widely applied to design thin MOF-based MMMs in liquid separation, especially for pervaporation.

Some porous substrates, such as polymeric membranes and ceramic tubes, were used to support the obtained MMMs and improve their stability and strength. The conventional procedure of this method involves three steps: (1) mixing the MOFs and polymer into the solvent (MOF ink); (2) casting the mixed solution on the porous support by spin-coating/dip-coating/flat membrane casting process; and (3) a curing or drying process to remove the casting solvent. With this procedure, thin MOF-based MMMs with a thickness of 0.3–20 mm are formed on the surface of a porous support.

An organophilic pervaporation membrane was fabricated on the inside surface of alumina capillary substrates by the solution-blending dip coating process, using ZIF-8 nanoparticles as filler and polymethylphenylsiloxane (PMPS) as polymer matrix [69]. After the heat-treatment process, the ZIF-8 nanoparticles were embedded in the PMPS phase homogeneously, with no interfacial voids. The top-layer thickness is about 2.5 mm, which may offer the possibility of achieving very high permeance.

Substrate-free blending presents more flexible applications in designing MOF-based MMMs. Nonporous supports were utilized to ensure the complete delamination from the substrate to create free-standing MMMs [68]. For better mechanical strength and permeance, the thickness of the membrane is generally controlled between 18 and 30 mm for pervaporation application, and larger than 150 mm for water treatment purpose. The substrate-free blending method was utilized to prepare a MIL-53(Al) nanocomposite using poly(*m*-phenylene isophthalamide) (PMIA, polymer) and MIL-53(Al) particles in a mixture of *N,N*-dimethylacetamide, and LiCl [70]. The membranes were placed in a vacuum oven before being immersed in distilled water to induce phase inversion process. However, the agglomeration of nanoparticles occurred. To overcome this, the postsynthetic approach was applied for more excellent dispersion of nanoparticles. A new, chemically crosslinked membrane with the application of postsynthetic polymerization of the UiO-66-NH<sub>2</sub> nanocrystals and polyurethane oligomer was developed [71]. The preparation of membrane involved the mixing of UiO-66-NH<sub>2</sub> particles with isocyanate-terminated polyurethane oligomer in anhydrous chloroform and was fully dispersed by ultrasound. The reacted solution was poured into a PTFE dish and allowed to dry at room temperature prior to being heated in an air-circulating oven. The obtained, well-dispersed MMMs showed the ability to isolate hydrophilic dyes from water by means of different membrane affinities.

### 7.2.1.5 Other design strategies

Apart from the aforementioned techniques, there are some other techniques reported for the preparation of MOF membranes. One of the techniques is the counterdiffusion method as reported by Kwon et al. [72]. This simple, yet highly versatile, method enabled the rapid preparation of well-intergrown ZIF-8 membranes on an alumina support with excellent microstructure. The synthesis method is basically the counterdiffusion concept in which a metal precursor solution is soaked in porous  $\alpha$ -alumina supports followed by rapid solvothermal reaction in a ligand solution. This novel method showed a significant effect on healing defects of membranes as well as to reduce ligands and solvents consumption. Fig. 7.8 shows the schematic illustration for the reaction.

As a measure to reduce the defect problems of ZIF-8 on the support surface, Jang et al. [73] reported on the new approach to control the diffusion rates of the two ZIF-8 precursors via the counterdiffusion method. The  $\gamma$ -Al<sub>2</sub>O<sub>3</sub> layer, with a pore size of 5 nm, was layered on top of the  $\alpha$ -Al<sub>2</sub>O<sub>3</sub> disc (referred to as a  $\gamma$ -/ $\alpha$ -Al<sub>2</sub>O<sub>3</sub> disc) as a tuner to

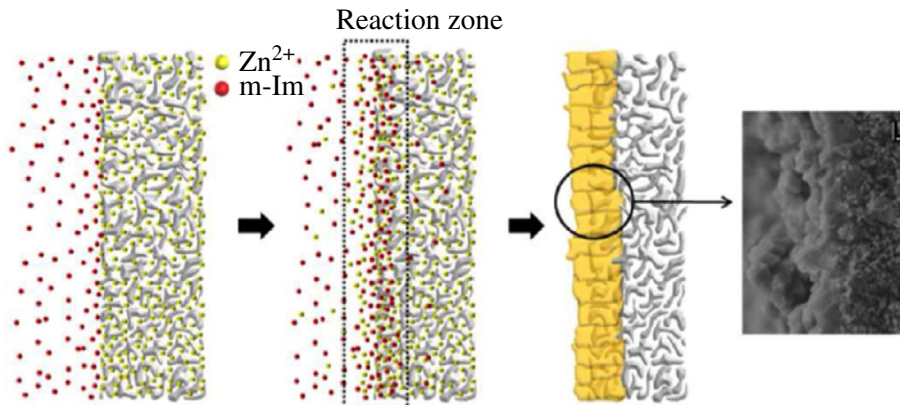


**Fig. 7.8** Schematic illustration of the membrane synthesis using the counterdiffusion-based in situ method: (1) a porous alumina support saturated with a metal precursor solution is placed in a ligand solution containing sodium formate, (2) the diffusion of metal ions and ligand molecules causes the formation of “reaction zone” at the interface (3) rapid heterogeneous nucleation/crystal growth in the vicinity at the interface leads to the continuous well-intergrown ZIF-8 membranes. Adapted with permission from H.T. Kwon, H.-K. Jeong, *In situ synthesis of thin zeolitic–imidazolate framework ZIF-8 membranes exhibiting exceptionally high propylene/propane separation*, *J. Am. Chem. Soc.* 135 (2013) 10763–10768. doi:10.1021/ja403849c.

decrease the diffusion rates. At the same time,  $\gamma$ -Al<sub>2</sub>O<sub>3</sub> also serves as a protective layer to prevent thermal structural damage to the ZIF-8 membranes. It was found that the ZIF-8 grains in membrane ZIF-8\_ $\gamma\alpha$  were predominantly formed inside the  $\alpha$ -Al<sub>2</sub>O<sub>3</sub> disc while filling  $\sim$ 70% of the mesopores in the  $\gamma$ -Al<sub>2</sub>O<sub>3</sub> layer. On the other hand, Li et al. [74] reported the synthesis of the ZIF-8 membrane using a solvothermal method on a porous alumina support. The support was initially immersed in 2-methylimidazole melting solution and then heated in a zinc nitrate aqueous solution through an infiltration method. A well-intergrown and continuous membrane was produced after 8 h at 120°C. The thickness of the membrane was about 12  $\mu$ m, and the highest zinc concentration was found at the surface.

Further, a novel pressure-assisted self-assembly (PASA) filtration technique was applied to prepare a MOF@GO membrane on a modified PAN support for pervaporation as shown in Fig. 7.9 [75]. The pretreated PAN support and the mixture of MOF and GO dispersion aqueous solution were installed in the membrane-preparation device. The PASA filtration process was operated at a constant pressure difference, DP = 2.0 bar, which induced the formation of a MOF@GO membrane.

These membranes exhibited competitive water permeation for ethyl acetate/water mixtures by pervaporation. Moreover, the procedures for both the synthesis of MOF and membrane preparation are environment friendly, as only water was used as a solvent. A nanosized MOF-intercalating approach like this may be extended to other laminated

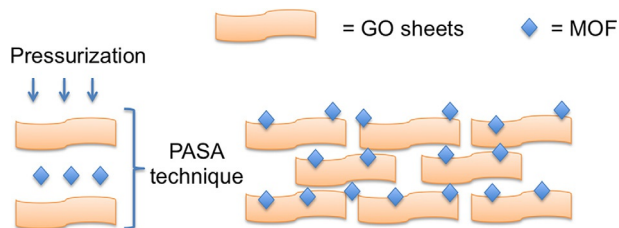


**Fig. 7.9** Pressure-assisted self-assembly (PASA) filtration technique to prepare a MOF@GO membrane on a modified PAN. Adapted with permission from Y. Ying, D. Liu, W. Zhang, H. Huang, Q. Yang, C. Zhong, *High-flux graphene oxide membranes intercalated by MOF with highly selective separation of aqueous organic solution, Appl. Mater. Interfaces* (2016). doi:10.1021/acsami.6b14371.

membranes, providing valuable insights into designing and developing advanced membranes for effective separation of aqueous organic solutions through nanostructure manipulation of the nanomaterials. More recently, inspired by the solvothermal synthesis of MOFs, the rapid thermal deposition (RTD) method to design a well-interconnected ZIF-8 membrane on a modified macroporous stainless steel substrate was reported [76]. Hmim solution was added to the zinc acetate solution in a dropwise manner to prepare the precursor solution. The precursor solution was then spread on the substrate in a crucible to initiate the crystallization of ZIF-8 across the substrate. RTD has been demonstrated as a much more efficient route, yielding a high-quality MOF membrane within 1 h, as opposed to the 24 h required for solvothermal membranes.

## 7.2.2 MOFs membrane application

### 7.2.2.1 Liquid separation

#### Pervaporation

MOF membranes for pervaporation is a natural extension of the current industry standards, considering the chemical versatility and subsequent separation tunability that is more freely available in comparison with polymeric or zeolites membranes [48]. For example, in the separation of water from ethanol, a hydrophilic MOF, known as HKUST-1 ( $\text{Cu}_3(\text{btc})_2$ ), was used in a 40 wt% mixed-matrix membrane (MMM) to remove water from the system [77]. Adding HKUST-1 improved flux without sacrificing selectivity due to the selective permeability of water in the membrane. Fig. 7.10 shows some typical MOFs used in pervaporation MMMs.

The applications of MOF-based membranes for pervaporation can be divided into four main categories: dehydration of organic solvents; removal of dilute organic compounds from aqueous streams; separation of organic-organic mixtures; and reversible reactions [68]. Due to the ease of design and modification of MOFs, along with the compatibility between MOFs and polymer matrix, MOF-based MMMs are superior in pervaporation compared to MMMs containing purely inorganic zeolites [37]. An integrated ZIF-71 membrane was prepared for the first time and used for pervaporation separation

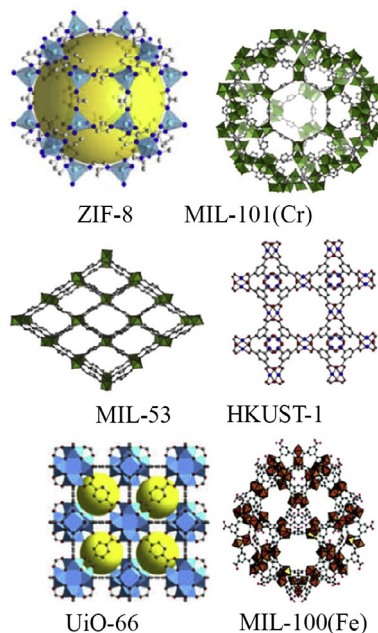


**Fig. 7.10** Structure of some typical MOFs used in pervaporation MMMs. Adapted with permission from Z. Jia, G. Wu, *Metal-organic frameworks based mixed matrix membranes for pervaporation*, *Microporous Mesoporous Mater.* 235 (2016) 151–159. doi:10.1016/j.micromeso.2016.08.008.

of alcohol (methanol and ethanol)–water and dimethyl carbonate (DMC)–methanol mixtures [78]. The kinetic diameter of ethanol (4.53 Å) is close to the window size of ZIF-71 (nominal 4.8 Å), which led to a relatively slower diffusion rate for ethanol molecules. In contrast, the diffusion of methanol (with a kinetic diameter of 3.63 Å) in the ZIF-71 channel is relatively fast, resulting in better separation performance. The ZIF-71 membrane shows good pervaporation performance, especially in DMC–methanol separation. The study also indicates that ZIF-71 pervaporation membranes demonstrate good performance not only for organics–water separation but for organics–organics systems as well.

Apart from that, a continuously grown  $\text{Ni}_2(\text{L-asp})_2\text{bipy}$  membrane was prepared on porous  $\text{SiO}_2$  discs by a seeding–secondary growth method, as shown in Fig. 7.11 [79]. The hydrophilic surface of the membrane was switched to hydrophobic by vapor deposition of PDMS, while the porosity was maintained even after the PDMS deposition. Pervaporation water/ethanol separation process was evaluated for both the PDMS-deposited membrane and the nondeposited PDMS membrane.  $\text{Ni}_2(\text{L-asp})_2\text{bipy}$  membrane possesses a remarkably high flux of  $27.6 \text{ kg m}^{-2} \text{ h}^{-1}$  and a separation factor of 73.6 for water/ethanol mixture with 50 wt% ethanol at the temperature of  $30^\circ\text{C}$ . The developed  $\text{Ni}_2(\text{L-asp})_2\text{bipy}@\text{PDMS}$  membrane exhibits a lower separation factor due

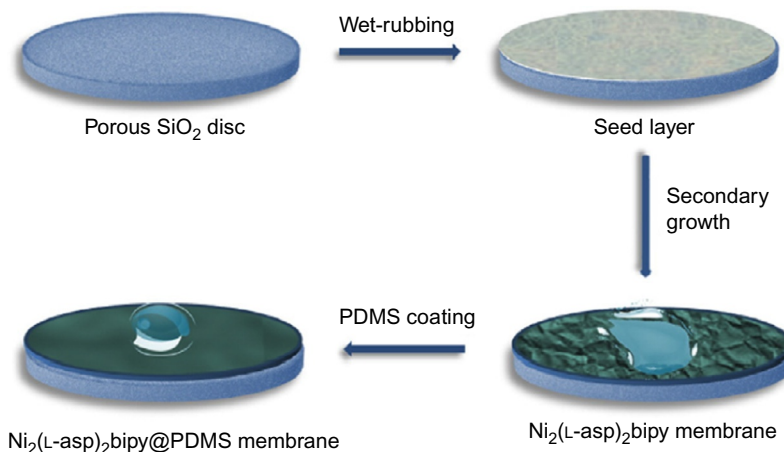


**Fig. 7.11** Schematic illustration of the preparation process of Ni<sub>2</sub>(L-asp)<sub>2</sub>bipy and Ni<sub>2</sub>(L-asp)<sub>2</sub>bipy@PDMS membranes and water/ethanol separation on them. Adapted with permission from S. Wang, Z. Kang, B. Xu, L. Fan, G. Li, L. Wen, X. Xin, Z. Xiao, J. Pang, X. Du, D. Sun, *Wettability switchable metal-organic framework membranes for pervaporation of water/ethanol mixtures*, *Inorg. Chem. Commun.* 82 (2017) 64–67. doi:10.1016/j.inoche.2017.05.016.

to its hydrophobic surface, which may be applied to the membrane distillation for water/ethanol separation. The pervaporation studies using these two membranes provide insight into the effect of surface wettability on the bioethanol purification performance [79].

A novel MOF nanocomposite membrane, with high loading rate and excellent stability, has been developed to increase the economic and process efficiency of current bio-refining processes, particularly for furfural (2-furancarboxaldehyde) refining process [80]. The membrane consists of a hierarchically ordered stainless-steel-mesh (HOSSM) that acts as a skeleton, while the ZIF-8 nanoparticle incorporated in the silicone rubber (PMPS) matrix create preferential pathways for furfural molecules by their ultrahigh adsorption selectivity. The HOSSM-ZIF-8-PMPS membrane shows very promising pervaporation and vapor permeation performance and excellent stability for the recovery and removal of furfural from dilute aqueous solution and biomass fermentation broth.

A well-intergrown UiO-66 MOFs membrane fabricated via controlled solvothermal synthesis on prestructures yttria-stabilized cations was applied in organic dehydration using pervaporation [81]. The membranes provide a very high flux of up to ca. 6.0 kg m<sup>-2</sup> h<sup>-1</sup> and an excellent separation factor for separating water from i-butanol (next-generation biofuel), furfural (promising biochemical), and tetrahydrofuran (typical organic matter). It is comparable to the performance of commercial zeolite NaA membranes and also showed better stability compared to some commercial membranes, such as zeolite NaA membranes. Recently, MIL-60 membranes were prepared on

polydopamine (PDA)-modified  $\alpha$ -Al<sub>2</sub>O<sub>3</sub> disks to separate xylene isomers via pervaporation [82]. A well intergrown MIL-160 crystal with a thickness of about 25  $\mu\text{m}$  was formed on the alumina support with no cracks or pinholes, suggesting a dense MIL-160 membrane had formed on the PDA-modified  $\alpha$ -Al<sub>2</sub>O<sub>3</sub> disk. The separation performance of the MIL-160 membrane was tested by the pervaporation of single components of PX, OX, and MX, as well as the separation of equimolar binary PX/OX mixture using liquid feeds. Membranes prepared on the nonmodified support show almost no selectivity (1.17 for PX/OX, and 1.13 for PX/MX). For the MIL-160 membrane prepared on the PDA-modified  $\alpha$ -Al<sub>2</sub>O<sub>3</sub> disk, the PX flux ( $486 \text{ g}^{-2} \text{ h}^{-1}$ ) is much higher than the flux of OX ( $10 \text{ g}^{-2} \text{ h}^{-1}$ ) and MX ( $12 \text{ g}^{-2} \text{ h}^{-1}$ ), with ideal separation factors of PX/OX and PX/MX being 48.6 and 40.5, respectively, indicating that the MIL-160 membranes prepared on the PDA-modified Al<sub>2</sub>O<sub>3</sub> disk display a high separation performance. The molecular sieving performance of the MIL-160 membrane was confirmed by the separation of equimolar PX/OX mixtures at 25–100°C by pervaporation. Comparing the PX flux in the mixture ( $467 \text{ g}^{-2} \text{ h}^{-1}$ ) with the flux of single component PX flux ( $486 \text{ g}^{-2} \text{ h}^{-1}$ ) at 75°C, only a slight reduction of the PX flux in the presence of OX is found, suggesting that the larger OX only slightly hinders the entrance of PX into the MIL-160 pore structure. For the 1:1 binary PX/OX mixture at 75°C, the mixture separation factor of PX/OX is 38.5, which is comparable to the PX/OX separation factor ( $\sim 40$ ) of the zeolite MFI membrane by pervaporation.

### Organic solvent nanofiltration

The good attributes of MOFs have attracted researchers to reveal their potential in other applications, including in OSN. The incorporation of [Cu<sub>3</sub>(BTC)<sub>2</sub>], MIL-47, MIL-53(Al), and ZIF-8 as fillers in PDMS membranes had been studied to separate Rose Bengal from isopropanol [83]. However, because of the poor adhesion between the MOFs and PDMS, the fillers were not successfully introduced into the polymer. The adhesion was improved by modifying the MOF surface with trimethylsilyl groups. The MMM showed increased permeance but lower retention compared to the pristine membrane due to the effect of reduced polymer swelling and size exclusion of the filler.

In 2013, Sorribas et al. prepared thin-film composite membranes containing MOF nanoparticles (ZIF-8, MIL-53(Al), NH<sub>2</sub>-MIL-53(Al), and MIL-101(Cr)) with the particle size of 50–150 nm in the PA layer via in situ polymerization on top of crosslinked polyimide porous support [84]. These membranes showed a dramatic increase in permeance when tested in MeOH/PS and THF/PS nanofiltration experiments compared to the same membranes with no MOFs, without sacrificing rejection. It was observed that there are direct trends between MeOH/PS permeance and the porosity of the MOFs added to the thin-film layer. The porosity of the MOFs provided preferential flow paths for the solvents, whereas the high rejection observed in this study was due to the excellent compatibility between PA and the organic moieties of the MOF particles. Mesoporous

MIL-101(Cr) showed the best performance with flux increases from 1.5 to 3.9 for MeOH/PS  $\text{m}^{-1} \text{h}^{-1} \text{bar}^{-1}$  and 1.7 to 11.1  $\text{L m}^{-1} \text{h}^{-1} \text{bar}^{-1}$  for THF/PS. The results proved that loading PA thin-film's separating layer with small amounts of MOFs significantly improved the flux without sacrificing rejection.

Nanoparticles of MOFs MIL-101(Cr), MIL-68(Al), and ZIF-11 with sizes of 70, 103, and 79 nm were also incorporated into an ultrathin PA layer from TFN membranes on top of polyimide P84<sup>®</sup> asymmetric support for OSN application [47]. Other important aspects that were also studied include the effect of a nonsolvent bath, chemical posttreatment, concentration of precursors of IP and the polymerization time, and the influence of different solvents (water, methanol, acetone, and THF) and solutes (Acridine Orange, Sunset Yellow, and Rose Bengal) on OSN. The results obtained showed that the hydrophilic character of the membranes had the most significant effect on the composite membrane's performance. Maximum permeance of  $6.2 \text{ L m}^{-2} \text{h}^{-1} \text{bar}^{-1}$  and a rejection above 90% was obtained from the combination of ZIF-11 and posttreatment via filtration with dimethylformamide because better MOF-polymer interaction was achieved, probably due to the hydrophobic character of ZIF-11.

In order to deal with selectivity issue, which is one of the main challenges problems in OSN, Campbell et al. [85] constructed membranes with uniform porous structure of HKUST-1 within the pores of polyimide membranes by using in situ growth method. Chemical modification was performed to improve the in situ growth membranes by introducing aryl carboxylic acid moieties (1,2,4-benzenetricarboxylic anhydride) to polyimide P86 ultrafiltration membranes, which then enabled coordination of HKUST-1 directly on the polymer. The results showed that chemically modified and HKUST-1 growth membrane exhibited better performance with a molecular weight cut-off of  $794 \text{ g mol}^{-1}$  and also high permeance [85].

Guo et al., prepared a defect-free TFN membrane by modifying the PA surface with long alkyl chains and in situ growth of zirconium-MOF (UiO-66-NH<sub>2</sub>) [86]. The modification of PA surface using dodecyl aldehyde improved the dispersibility of nanosized UiO-66-NH<sub>2</sub> particles ( $\sim 20 \text{ nm}$ ) in hexane and enhanced the compatibility with the polymer phase, leading to nonselective defects in ultrathin MOF@PA TFN membrane. Methanol permeance was enhanced significantly after nanoparticle incorporation without compromising the tetracycline rejection. The novel TFN membrane prepared with organic phase solution containing 0.15% (w/v) modified UiO-66-NH<sub>2</sub> showed remarkable methanol permeance of  $20 \text{ L m}^{-2} \text{h}^{-1} \text{bar}^{-1}$ , with tetracycline rejection of 99%, suggesting promise for application in the pharmaceutical industry.

Li et al. proposed another approach to incorporate MOF into polymeric membranes through an IP method inspired by traditional RO membrane fabrication [52]. Through the applied method, PES was first saturated with the aqueous zinc nitrate followed by 2-methylimidazole dissolved in octanol and left for certain reaction times for the ZIF-8 to form. The results indicated that higher concentrations and higher mole ratios

of 2-methylimidazole to zinc nitrate led to denser ZIF-8 membranes with fewer defects. However, due to the dense packing and smaller interparticle spaces, the changes also affected the permeance and rejection of the membrane. It is very clear that the higher 2-methylimidazole and zinc nitrate molar ratios resulted in much denser films with lower permeance. By changing the molar ratio of 2-methylimidazole to zinc nitrate from 1.9 to 15.9, ZIF-8/the permeance PES membranes varied from 5.6 to 37.5 L m<sup>-2</sup> h<sup>-1</sup> bar<sup>-1</sup>, with Rose Bengal rejections higher than 98%.

A study involving the incorporation of ZIF-8 onto the surface of Graphene Oxide to form ZIF-8@GO composite determined the potential of the materials for OSN [87]. ZIF-8@GO nanoparticles were codeposited with polyethyleneimine (PEI) matrix on a tubular ceramic substrate through a vacuum-assisted assembly method. The method showed improved dispersion of ZIF-8 nanoparticles in a PEI matrix, as well as its compactness due to the tinplating effect of lamellar GO sheets and the transmembrane pressure. The OSN performance was evaluated on the basis of methanol permeance and retention of dye molecules. Methanol permeance increased when ZIF-8@GO laminates were embedded into the PEI layer. The retention remained higher than 99%. The excellent performance of the membrane may be due to the more well-defined pathways for solvent molecules provided by the good dispersion of ZIF-8 nanoparticles in the PEI matrix.

### Water treatment

A growing number of industrial applications use membrane-based separations. The emergence of MOFs has given new insight and might greatly improve the performance and the range of membrane separations that are possible [68]. There have been numerous studies on the preparation and promising performance of MOFs acting as continuous membranes or fillers in MMMs for nanofiltration, forward osmosis, ultrafiltration, and reverse osmosis application. The introduction of MOFs into membrane-based separations gives multifunctional effects for water treatment processes, for instance, catalytic degradation, heavy metal removal, and antibacterial properties. Since the size of an MOF's pore window can range from 0.3 to 10 nm, depending on the composition, MOF membranes usually served as nanofiltration membranes. They compete with the RO membrane in term of performance.

The use of MOF-based membranes in nanofiltration is mainly focused on dye removal. A novel LBL PA/ZIF-8 nanocomposite membrane was fabricated to overcome the aggregation of fillers, which lead to a significant decrease in membrane performance [88]. The multilayer membrane consists of a porous substrate, a ZIF-8 interlayer, and a PA coating layer, as shown in Fig. 7.11. An interlayer of ZIF-8 was grown on an ultrafiltration membrane through in situ growth, and the layer was coated with an ultrathin PA layer through interfacial polymerization (IP). The LBL PA/ZIF-8 showed better performance than the conventional PA/ZIF-8 TFN membrane because the in situ growth

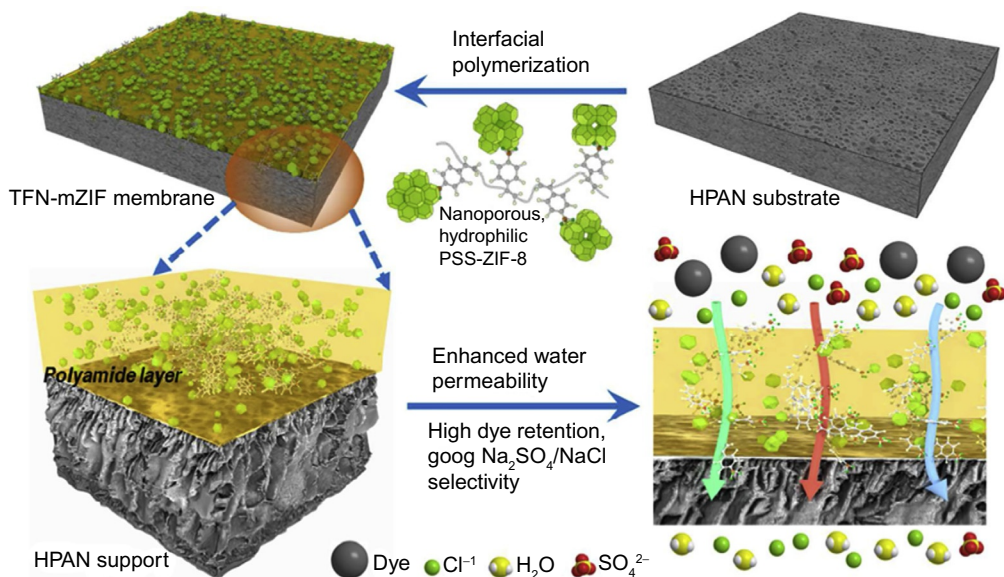


**Fig. 7.12** Preparation of PSS-ZIF-8 membrane through IP and water permeability and selectivity of molecules. Adapted with permission from Z. Junyong, Q. Lijuan, U. Andrew, J. Hou, W. Jing, Zh. Yatao, L. Xin, Y. Shushan, L. Jian, T. Miaomiao, L. Jiuyang, B. Van Der Bruggen, *Elevated performance of thin film nanocomposite membranes enabled by modified hydrophilic MOFs for nanofiltration*, *ACS Appl. Mater. Interfaces* (2016). doi:10.1021/acsami.6b14412.

of ZIF-8 produces an interlayer with more particles and fewer aggregates. LBL PA/ZIF-8 performed better permeance and selectivity for dye removal with flux was up to  $27.1 \text{ kg m}^{-2} \text{ h}^{-1}$ , and the rejection reaches 99.8% compared to the pure PA membrane (flux of  $11.2 \text{ kg m}^{-2} \text{ h}^{-1}$  and rejection of 99.6%).

Apart from direct dyes, MOF-based membranes can also remove reactive dyes such as Reactive Blue 2 (RB2) and Reactive Black 5 (RB5). TFC and TFN ZIF-8 membranes display high retention for both dyes, which meets the prime separation requirement of NF membranes [89]. The preparation of membrane and molecular sieving through the membrane is shown in Fig. 7.12. Although lower dye retentions were measured than those for TFC (RB2: 99.42%, RB5: 99.92% compared to TFN-mZIF2 RB2: 99.12, RB5: 99.03), the water flux of TFN-mZIF2 was enhanced by 199.3% at 4 bar, which is promising for dye removal.

A membrane derived from ZIF-8/PSS, based on a tubular alumina substrate through LBL self-assembly technique, was fabricated for nanofiltrating dyes from water [55]. The ZIF-8 particles were grown in situ into PSS layers to enhance compatibility and dispersion. In the study, there were outstanding nanofiltration properties toward methyl blue with the flux of  $210 \text{ L m}^{-2} \text{ h}^{-1} \text{ MPa}^{-1}$  and the rejection of 98.6%. Additionally, the

membrane showed good pressure resistance because of the ceramic substance and inherent stability of ZIF-8.

On the other hand, two different types of TFC membranes with ZIF-8 were prepared, one in PA with PSF support, fabricated through IP, the other one was in situ growth on PSF support with PA as top layer prepared through the LBL technique [90]. The membranes were tested for the common analgesic acetaminophen (or paracetamol MW 151 g mol<sup>-1</sup>). Due to the membrane's defect-free characteristics, LBL membrane produced better performance with 55% acetaminophen retention and permeance equivalent to conventional PSF/PA membrane when compared to the membrane prepared through IP.

A new metal-organic framework/graphene oxide composite (IRMOF-3/GO) with high adsorption capacity of copper (II) was prepared with maximal adsorption of 254.14 mg g<sup>-1</sup> at pH 5.0 at room temperature [91]. Novel and highly efficient nanofiltration (NF) membranes can be readily fabricated via surface decoration of IRMOF-3/GO onto polydopamine (PDA)-coated polysulfone (PSF) substrate. The adsorption effect of IRMOF-3/GO and the enhancement of membrane caused the prepared NF membrane efficiently reject copper (II). The copper (II) rejection reached up to about 90% while maintaining a flux of about 31 L m<sup>-2</sup> h<sup>-1</sup> at the pressure of 0.7 MPa and pH 5.0. Furthermore, the membrane also maintains outstanding stability throughout a 2000-min NF testing period. Thus, the newly developed NF membrane shows promise for water-cleaning applications.

Duan et al. prepared an advanced RO membrane by integrating MOFs within the PA layer to produce a MOF-based TFN structure for the desalination process [92]. The TFN membranes were characterized with RO tests fewer than 15.5 bar hydraulic pressure with 2000 ppm NaCl solution. ZIF-8 increased the water permeance up to 3.35 ± 0.08 L m<sup>-2</sup> h<sup>-1</sup> bar<sup>-1</sup> at 0.4% (w/v) loading, 162% higher than the pristine PA membrane. Further, a high NaCl rejection was maintained. This study experimentally verified the potential use of ZIF-8 in advanced TFN RO membranes. Furthermore, due to their unique structural components, which contain metal cores and organic ligands, MOFs have also exhibited remarkable antimicrobial properties. The antimicrobial property of the MOF-based membrane was also achieved by functionalizing a TFN membrane with ZIF/GO hybrid nanosheets [55]. The resultant hybrid nanosheets not only integrated the merits of both ZIF-8 and GO but also yielded a uniform dispersion of ZIF-8 onto GO nanosheets simultaneously, thus effectively eliminating the agglomeration of ZIF-8 in the active layer of membranes. ZIF-8/GO thin-film nanocomposites (TFN-ZG) membrane with typical water permeability (40.63 L m<sup>-2</sup> h<sup>-1</sup> MPa<sup>-1</sup>) allowed for efficient bivalent salts removal with the rejections of Na<sub>2</sub>SO<sub>4</sub> and MgSO<sub>4</sub> were 100% and 77%, respectively. Interestingly, the synthesized ZIF-8/GO nanocomposites had optimal antimicrobial activity (MIC: 128 µg mL<sup>-1</sup>), compared to ZIF-8 and GO separately, which sufficiently contributed to the excellent microbial activity

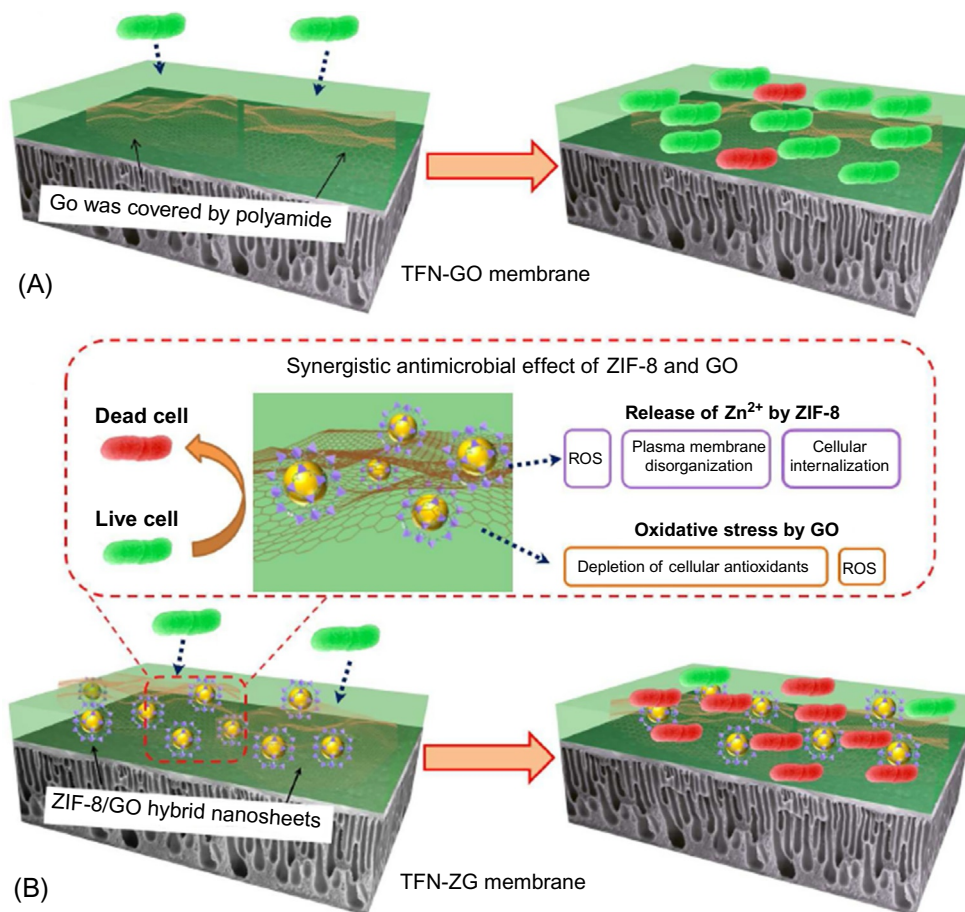


**Fig. 7.13** (A) Schematic diagrams for the antimicrobial mechanism of TFN-GO membranes and (B) TFN-ZG membranes. Adapted with permission from J. Wang, Y. Wang, Y. Zhang, A. Uliana, J. Zhu, J. Liu, B. Van Der Bruggen, Zeolitic Imidazolate framework/graphene oxide hybrid nanosheets functionalized thin film nanocomposite membrane for enhanced antimicrobial performance, *ACS Appl. Mater. Interfaces* 8 (2016) 25508–25519. doi:10.1021/acsami.6b06992.

of TFN-ZG (84.3%). The antimicrobial mechanisms of ZIF-8/GO hybrid nanosheets and TFN-ZG membranes were proposed, as shown in Fig. 7.13. ZIF-8/GO functionalized membrane with high antimicrobial activity, and salt retention makes it promising for water desalination, and it was suggested that ZIF-8-based crystal may offer a new pathway for the synthesis of multifunctional bactericidal. The potential antimicrobial mechanism of the ZIF-8/GO membrane is attributed to a synergistic effect involving graphene oxide and the gradual releasing of Zn<sup>2+</sup> from ZIF-8. This research suggests a promising future for ZIF-8-based nanocomposites as multifunctional antimicrobial agents for versatile applications.

### 7.2.2.2 Gas separation

Porous materials separate gases based on differences in diffusion coefficients or by a molecular sieving effect between the gases and porous material [48]. Many MOF membranes and MOF-polymer composite membranes have been explored for their potential application in gas separation. Among the many gases studied for separation by MOFs, the separation of CO<sub>2</sub> from flue gas streams has become a major area of interest because of its relevance to climate change and the fact that many different MOFs have shown high selectivity for CO<sub>2</sub> uptake [93]. For example, a high-quality isorecticular MOF-1 (IRMOF-1) membrane was prepared for the separation of CO<sub>2</sub> from dry CO<sub>2</sub>-enriched CO<sub>2</sub>/CH<sub>4</sub> and CO<sub>2</sub>/N<sub>2</sub> mixture [94]. The membrane exhibits good separation for CO<sub>2</sub>/CH<sub>4</sub> and CO<sub>2</sub>/N<sub>2</sub> with separation factors of 328 and 410, respectively. The CO<sub>2</sub> permeance reported for CO<sub>2</sub>/CH<sub>4</sub> and CO<sub>2</sub>/CH<sub>4</sub> is  $2.55 \times 10^{-7}$  and  $2.06 \times 10^{-7}$ , respectively. The unique separation properties of IRMOF-1 membranes, such as “sharp molecular sieving” at high CO<sub>2</sub> molar fraction and feed pressure and high CO<sub>2</sub> permeance, could contribute to the production of high-purity CO<sub>2</sub> from the low-grade CO<sub>2</sub> gas mixtures. Mixed matrix membranes (MMM) well-dispersed MOF fillers in polymer matrices were prepared via thermally induced oxidative crosslinking of the polymer matrix and the amorphized zeolitic imidazolate framework [95]. The resultant plasticization-resistant MMMs exhibited high selective separations for CO<sub>2</sub>/CH<sub>4</sub> mixed gas feeds. The membrane could also serve as molecular sieves for other separation processes, such as pervaporation or OSN. Apart from CO<sub>2</sub>, another important gas is hydrogen (H<sub>2</sub>) because it could fulfill the world’s increasing energy requirements in an environment-friendly manner [96]. MOF-based membrane has shown potential for hydrogen separation [97].

The first MOF-based membrane reported consisted of an MOF-5 membrane fabricated using an in situ solvothermal method on top of alumina support [98]. The single gas permeation properties demonstrated that they follow Knudsen diffusion behavior. As the permeation rate of gases increases by a decrease in their molecular weight, H<sub>2</sub>, which has the lowest molecular weight, permeates faster than the heavier studied gases, like CH<sub>4</sub>, N<sub>2</sub>, CO<sub>2</sub>, and SF<sub>6</sub>. This phenomenon suggests that the pore-aperture size of MOF-5 is larger than all of the tested molecules in this case.

Another MOF membrane, HKUST-1 MOF (also known as Cu<sub>3</sub>(btc)<sub>2</sub> or MOF-199), was grown using the “twin copper source” solvothermal method [99]. HKUST-1 MOF has small cages structure with diameters of 13 and 10 Å, accessible through windows of ca. 11 and 9.3 Å, respectively. High permeation flux of single gas permeation test was expected due to the pore-aperture size of HKUST-1, which is greater than the kinetic diameter of the commonly studied gases. The permeation results also showed a permeation selectivity in favor of H<sub>2</sub> with respect to other gases, such as H<sub>2</sub>/N<sub>2</sub> = 7, H<sub>2</sub>/CO<sub>2</sub> = 6.8, and H<sub>2</sub>/CH<sub>4</sub> = 5.9. On the other hand, another HKUST-1 membrane was prepared through LBL approach, firstly by seeding process

followed by in situ solvothermal method. The single gas separation performances for this membrane were also evaluated, and the ideal selectivities of this membrane were 2.9, 3.7, and 5.1 for  $\text{H}_2/\text{CH}_4$ ,  $\text{H}_2/\text{N}_2$ , and  $\text{H}_2/\text{CO}_2$ , respectively. These ideal selectivities indicate that the permeation behavior of this membrane follows the Knudsen diffusion.

Another group of MOFs, which is known as ZIFs, also showed good performance for hydrogen separation. The unique properties of ZIFs, in terms of permanent porosity, pore-aperture size uniformity, and excellent chemical and thermal stability made them good candidates for their application as molecular sieve membranes [96]. Among all ZIFs, ZIF-8 is one of the most studied. It has an underlying topology with 3.4 Å aperture size for the six-membered-ring as the sole entrance to the associated pores. Theoretically, this could separate  $\text{H}_2$  from the other larger associated gases. A ZIF-8 membrane for gas separation with selectivity for  $\text{H}_2$  was obtained via a novel microwave-assisted solvothermal process [100]. The membrane single-gas permeation results of this ZIF-8 membrane showed a higher  $\text{H}_2/\text{CH}_4$  selectivity of 11.2, relative to MOF membranes reported earlier.

### 7.3 Conclusions

The emergences of zeolites and MOFs have given new insights into the development of membrane technologies, particularly for liquid and gas separation. The promising characteristics of both materials in term of surface area, tunability, chemical, and structural design make them suitable candidates for membrane separation applications. Progressive research on the fabrication and performance of zeolites and MOFs membrane have led to a greater number of new methods to produce defect-free membranes for better performance. Despite the tremendous progress, some significant challenges remain with respect to the implementation of zeolites and MOF membranes for industrial application. The challenges include, but are not limited to, the demand for easy membrane development, inexpensive supports, and low-cost methods for large-scale fabrication. To meet the requirements of industrial demands, research efforts need to expand.

### References

- [1] J. Weitkamp, Zeolites and catalysis, *Solid State Ionics* 131 (2000) 175–188, <https://doi.org/10.1002/9783527630295>.
- [2] A. Tavoraro, E. Drioli, Zeolite membranes, *Adv. Mater.* 11 (1999) 975–996, [https://doi.org/10.1002/\(SICI\)1521-4095\(199908\)11:12](https://doi.org/10.1002/(SICI)1521-4095(199908)11:12).
- [3] K.T. Jung, Y.G. Shul, Preparation of transparent TS-1 zeolite film by using nanosized TS-1 particles, *Chem. Mater.* 4756 (1997) 420–422.
- [4] H. Xu, D.B. Shah, O. Talu, Synthesis of ZSM-5 films at elevated gravity, *Zeolites* 2449 (1997) 114–122.
- [5] Y. He, X.M. Cui, X.D. Liu, Y.P. Wang, J. Zhang, K. Liu, Preparation of self-supporting NaA zeolite membranes using geopolymers, *J. Membr. Sci.* 447 (2013) 66–72, <https://doi.org/10.1016/j.memsci.2013.07.027>.

- [6] J. Zhang, Y. He, Y.P. Wang, J. Mao, X.M. Cui, Synthesis of a self-supporting faujasite zeolite membrane using geopolymer gel for separation of alcohol/water mixture, *Mater. Lett.* 116 (2014) 167–170, <https://doi.org/10.1016/j.matlet.2013.11.008>.
- [7] T. Sano, Y. Kiyozumi, M. Kawamura, F. Mizukami, H. Takaya, T. Mouri, W. Inaoka, Y. Toida, M. Watanabe, K. Toyoda, Preparation and characterization of ZSM-5 zeolite film, *Zeolites* 11 (1991) 842–845, [https://doi.org/10.1016/S0144-2449\(05\)80066-1](https://doi.org/10.1016/S0144-2449(05)80066-1).
- [8] T. Sano, Y. Kiyozumi, K. Maeda, M. Toba, S.I. Niwa, F. Mizukami, New preparation method for highly siliceous zeolite films, *J. Mater. Chem.* 2 (1992) 141–142, <https://doi.org/10.1039/JM9920200141>.
- [9] M.W. Anderson, K.S. Pachis, J. Shi, S.W. Carr, Synthesis of self-supporting zeolite films, *J. Mater. Chem.* 2 (1992) 255–256.
- [10] S. Yamazaki, K. Tsutsumi, Adsorption characteristics of synthesized mordenite membranes, *Adsorption* 3 (1997) 165–171, <https://doi.org/10.1007/BF01650239>.
- [11] M. Kazemimoghadam, Preparation of self-supported HS zeolite membranes by a new method, *J. Ceram. Process. Res.* 17 (2016) 978–984.
- [12] W.J.W. Bakker, F. Kapteijn, J. Poppe, J.A. Moulijn, Permeation characteristics of a metal-supported silicalite-1 zeolite membrane, *J. Membr. Sci.* 117 (1996) 57–78, [https://doi.org/10.1016/0376-7388\(96\)00035-X](https://doi.org/10.1016/0376-7388(96)00035-X).
- [13] A.S. Huang, J. Liu, Y.S. Li, Y.S. Lin, W.S. Yang, Preparation of A-type zeolite membranes on non-porous metal supports by using electrophoretic technique, *Chin. Sci. Bull.* 49 (2004) 1226–1230, <https://doi.org/10.1360/04wb0010>.
- [14] J. Zhang, W. Liu, Thin porous metal sheet-supported NaA zeolite membrane for water/ethanol separation, *J. Membr. Sci.* 371 (2011) 197–210, <https://doi.org/10.1016/j.memsci.2011.01.032>.
- [15] A. Farjoo, S.M. Kuznicki, M. Sadrzadeh, Hydrogen separation by natural zeolite composite membranes: single and multicomponent gas transport, *Materials (Basel)* 10 (2017) 1–14, <https://doi.org/10.3390/ma10101159>.
- [16] A.K. Basumatary, R. Vinoth Kumar, K. Pakshirajan, G. Pugazhenthii, Removal of trivalent metal ions from aqueous solution via cross-flow ultrafiltration system using zeolite membranes, *J. Water Reuse Desalin.* 7 (2017) 66–76, <https://doi.org/10.2166/wrd.2016.211>.
- [17] A.d.S. Barbosa, A.d.S. Barbosa, T.L.A. Barbosa, M.G.F. Rodrigues, Synthesis of zeolite membrane (NaY/alumina): effect of precursor of ceramic support and its application in the process of oil–water separation, *Sep. Purif. Technol.* 200 (2018) 141–154, <https://doi.org/10.1016/j.seppur.2018.02.001>.
- [18] Z. Xu, Q. Chen, G. Lu, Preparation of zeolite X membranes on porous ceramic substrates with zeolite seeds, *J. Nat. Gas Chem.* 11 (2002) 171–179.
- [19] M.K. Naskar, D. Kundu, M. Chatterjee, Silicalite-1 zeolite membranes on unmodified and modified surfaces of ceramic supports: a comparative study, *Bull. Mater. Sci.* 32 (2009) 537–541, <https://doi.org/10.1007/s12034-009-0080-2>.
- [20] X. Yao-Yi, W. Xue-Ling, L. Shuai, S. A-Li, C. Zi-Sheng, Synthesis of ZSM-5/NaA hybrid zeolite membrane using kaolin as modified layer, *New J. Chem.* (2018)C7NJ04953F <https://doi.org/10.1039/C7NJ04953F>.
- [21] A. Evcin, O. Tutkun, Preparation of Zeolite-Filled Polymeric Membranes for Pervaporation, in: *Preparation of Zeolite-Filled Polymeric Membranes for Pervaporation Materials are Also Reported, Such as Polyacrylonitrile (PAN), Variety of Organic Polymers, There Have Been Problems*, 2005.
- [22] J.-M. Duval, A.J.B. Kemperman, B. Folkers, M.H.V. Mulder, G. Desgrandchamps, C.A. Smolders, Preparation of zeolite filled glassy polymer membranes, *J. Appl. Polym. Sci.* 54 (1994) 409–418, <https://doi.org/10.1002/app.1994.070540401>.
- [23] H. Sudhakar, Y. Maruthi, U.S.K. Rao, C.V. Prasad, M.C.S. Subha, S. Sridhar, K.C. Rao, Improved pervaporation performance of 13X zeolite filled chitosan membranes, *Indian J. Adv. Chem. Sci.* 2 (2013) 21–31.
- [24] R.S. Murali, T. Sankarshana, S. Sridhar, Air separation by polymer-based membrane technology air separation by polymer-based membrane, *Sep. Purif. Rev.* 42 (2013) 130–186, <https://doi.org/10.1080/15422119.2012.686000>.

- [25] N.W. Ockwig, T.M. Nenoff, Membranes for hydrogen separation, *Chem. Rev.* 107 (2007) 4078–4110.
- [26] R. Faiz, K. Li, Olefin/paraffin separation using membrane based facilitated transport/chemical absorption techniques, *Chem. Eng. Sci.* 73 (2012) 261–284, <https://doi.org/10.1016/j.ces.2012.01.037>.
- [27] Y. Zhang, J. Sunarso, S. Liu, R. Wang, Current status and development of membranes for CO<sub>2</sub>/CH<sub>4</sub> separation: a review, *Int. J. Greenhouse Gas Control* 12 (2013) 84–107, <https://doi.org/10.1016/j.ijggc.2012.10.009>.
- [28] R. Bedard, C. Liu, Recent advances in zeolitic membranes, *Annu. Rev. Mater. Res.* (2018) 83–110, <https://doi.org/10.1146/annurev-matsci-070317>.
- [29] W. Zhu, P. Hrabanek, L. Gora, F. Kapteijn, J.A. Moulijn, Role of adsorption in the permeation of CH<sub>4</sub> and CO<sub>2</sub> through a silicalite-1 membrane, *Ind. Eng. Chem. Res.* 45 (2006) 767–776.
- [30] M.R. Othman, S.C. Tan, S. Bhatia, Separability of carbon dioxide from methane using MFI zeolite–silica film deposited on gamma-alumina support, *Microporous Mesoporous Mater.* 121 (2009) 138–144, <https://doi.org/10.1016/j.micromeso.2009.01.019>.
- [31] J.C. Poshusta, R.D. Noble, J.L. Falconer, Temperature and pressure effects on CO<sub>2</sub> and CH<sub>4</sub> permeation through MFI zeolite membranes, *J. Membr. Sci.* 160 (1999) 115–125.
- [32] M.A. Carreon, S. Li, J.L. Falconer, R.D. Noble, Alumina-supported SAPO-34 membranes for CO<sub>2</sub>/CH<sub>4</sub> separation, *J. Am. Chem. Soc.* 130 (2008) 5412–5413.
- [33] Y. Huang, L. Wang, Z. Song, S. Li, M. Yu, Growth of high-quality, thickness-reduced zeolite membranes towards N<sub>2</sub>/CH<sub>4</sub> separation using high-aspect-ratio seeds, *Angew. Chem. Int. Ed.* 54 (2015) 10843–10847, <https://doi.org/10.1002/anie.201503782>.
- [34] H. Shi, Organic template-free synthesis of SAPO-34 molecular sieve membranes for CO<sub>2</sub>–CH<sub>4</sub> separation, *RSC Adv.* 1 (2015) 38330–38333, <https://doi.org/10.1039/c5ra04848f>.
- [35] L. Liang, M. Zhu, L. Chen, C. Zhong, Y. Yang, T. Wu, H. Wang, I. Kumakiri, X. Chen, H. Kita, Single gas permeance performance of high silica SSZ-13 zeolite membranes, *Membranes (Basel)* (2018) 1–11, <https://doi.org/10.3390/membranes8030043>.
- [36] M.J. Vaezi, A.A. Babaluo, H. Maghsoudi, A.D.A. Eda, Separation of CO<sub>2</sub> and N<sub>2</sub> from CH<sub>4</sub> using modified DD3R zeolite membrane: a comparative study of synthesis procedures, *Chem. Eng. Res. Des.* 134 (2018) 347–358, <https://doi.org/10.1016/j.cherd.2018.03.004>.
- [37] Z. Jia, G. Wu, Metal-organic frameworks based mixed matrix membranes for pervaporation, *Microporous Mesoporous Mater.* 235 (2016) 151–159, <https://doi.org/10.1016/j.micromeso.2016.08.008>.
- [38] D.A. Fedosov, A.V. Smirnov, E.E. Knyazeva, I.I. Ivanova, Zeolite membranes: synthesis, properties, and application, *Pet. Chem.* 51 (2011) 657–667, <https://doi.org/10.1134/S0965544111080032>.
- [39] Y. Morigami, M. Kondo, J. Abe, H. Kita, K. Okamoto, The first large-scale pervaporation plant using tubular-type with zeolite NaA membrane, *Sep. Purif. Technol.* 205 (2001) 251–260, [https://doi.org/10.1016/S1383-5866\(01\)00109-5](https://doi.org/10.1016/S1383-5866(01)00109-5).
- [40] J. Caro, M. Noack, P. Kolsch, Zeolite membranes: from the laboratory scale to technical applications, *Adsorption* 44 (2005) 215–227.
- [41] M. Kazemimoghadam, New nanopore zeolite membranes for water treatment, *Desalination* 251 (2010) 176–180, <https://doi.org/10.1016/j.desal.2009.11.036>.
- [42] B. Zhu, D.T. Myat, J.W. Shin, Y.H. Na, I.S. Moon, G. Connor, S. Maeda, G. Morris, S. Gray, M. Duke, Application of robust MFI-type zeolite membrane for desalination of saline wastewater, *J. Membr. Sci.* 475 (2015) 167–174, <https://doi.org/10.1016/j.memsci.2014.09.058>.
- [43] H. Huang, Q. Xinying, J. Xiaosheng, G. Xin, Z. Lin, C. Haunlin, H. Lian, Acid and multivalent ion resistance of thin film nanocomposite RO membranes loaded with silicalite-1, *J. Mater. Chem. A* (2013) 11343–11349, <https://doi.org/10.1039/c3ta12199b>.
- [44] A.K. Basumatary, P.P. Adhikari, A.K. Ghoshal, G. Pugazhenthii, Fabrication and performance evaluation of faujasite zeolite composite ultrafiltration membrane by separation of trivalent ions from aqueous solution, *Environ. Prog. Sustain. Energy* 35 (2016) 1047–1054, <https://doi.org/10.1002/ep>.

- [45] Y. Yurekli, Removal of heavy metals in wastewater by using zeolite nano-particles impregnated polysulfone membranes, *J. Hazard. Mater.* 309 (2016) 53–64, <https://doi.org/10.1016/j.jhazmat.2016.01.064>.
- [46] O. Shekha, J. Liu, R.A. Fischer, C. Wöll, MOF thin films: existing and future applications, *Chem. Soc. Rev.* 40 (2011) 1081, <https://doi.org/10.1039/c0cs00147c>.
- [47] C. Echaide-Gorritz, S. Sorribas, C. Tellez, J. Coronas, MOF nanoparticles of MIL-68(Al), MIL-101 (Cr) and ZIF-11 for thin film nanocomposite organic solvent nanofiltration membranes, *RSC Adv.* (2016) 90417–90426, <https://doi.org/10.1039/C6RA17522H>.
- [48] M.S. Denny Jr., J.C. Moreton, L. Benz, S.M. Cohen, Metal–organic frameworks for membrane-based separations, *Nat. Rev. Mater.* 1 (2016) 1–17, <https://doi.org/10.1038/natrevmats2016.78>.
- [49] M. Shah, M.C. McCarthy, S. Sachdeva, A.K. Lee, H.K. Jeong, Current status of metal–organic framework membranes for gas separations: promises and challenges, *Ind. Eng. Chem. Res.* 51 (2012) 2179–2199, <https://doi.org/10.1021/ie202038m>.
- [50] H. Bux, A. Feldhoff, J. Cravillon, M. Wiebcke, Y.S. Li, J. Caro, Oriented zeolitic imidazolate framework-8 membrane with sharp H<sub>2</sub>/C<sub>3</sub>H<sub>8</sub> molecular sieve separation, *Chem. Mater.* 23 (2011) 2262–2269, <https://doi.org/10.1021/cm200555s>.
- [51] G. Xu, J. Yao, K. Wang, L. He, P.A. Webley, C. sheng Chen, H. Wang, Preparation of ZIF-8 membranes supported on ceramic hollow fibers from a concentrated synthesis gel, *J. Membr. Sci.* 385–386 (2011) 187–193, <https://doi.org/10.1016/j.memsci.2011.09.040>.
- [52] Y. Li, L.H. Wee, J.A. Martens, I.F.J. Vankelecom, Interfacial synthesis of ZIF-8 membranes with improved nanofiltration performance, *J. Membr. Sci.* 523 (2017) 561–566, <https://doi.org/10.1016/j.memsci.2016.09.065>.
- [53] M.C. McCarthy, V. Varela-Guerrero, G.V. Barnett, H.K. Jeong, Synthesis of zeolitic imidazolate framework films and membranes with controlled microstructures, *Langmuir* 26 (2010) 14636–14641, <https://doi.org/10.1021/la102409e>.
- [54] X. Zhang, Y. Liu, L. Kong, H. Liu, J. Qiu, W. Han, L.-T. Weng, K.L. Yeung, W. Zhu, A simple and scalable method for preparing low-defect ZIF-8 tubular membranes, *J. Mater. Chem. A* 1 (2013) 10635 <https://doi.org/10.1039/c3ta12234d>.
- [55] X. Wang, M. Sun, B. Meng, X. Tan, J. Liu, S. Wang, S. Liu, Formation of continuous and highly permeable ZIF-8 membranes on porous alumina and zinc oxide hollow fibers, *Chem. Commun.* 52 (2016) 13448–13451, <https://doi.org/10.1039/C6CC06589A>.
- [56] C. Algieri, G. Golemme, S. Kallus, J.D.F. Ramsay, Preparation of thin supported MFI membranes by *in situ* nucleation and secondary growth, *Microporous Mesoporous Mater.* 47 (2001) 127–134, [https://doi.org/10.1016/S1387-1811\(01\)00393-6](https://doi.org/10.1016/S1387-1811(01)00393-6).
- [57] L.S. Lai, Y.F. Yeong, K.K. Lau, A.M. Shariff, Effect of synthesis parameters on the formation of ZIF-8 under microwave-assisted solvothermal, *Procedia Eng.* 148 (2016) 35–42, <https://doi.org/10.1016/j.proeng.2016.06.481>.
- [58] Y. Pan, B. Wang, Z. Lai, Synthesis of ceramic hollow fiber supported zeolitic imidazolate framework-8 (ZIF-8) membranes with high hydrogen permeability, *J. Membr. Sci.* 421–422 (2012) 292–298, <https://doi.org/10.1016/j.memsci.2012.07.028>.
- [59] L.S. Lai, Y.F. Yeong, K.K. Lau, M.S. Azmi, Preliminary study on the synthesis of ZIF-8 membranes via *in situ* and secondary seeded growth methods, *Adv. Mater. Res.* 1133 (2016) 649–653, <https://doi.org/10.4028/www.scientific.net/AMR.1133.649>.
- [60] K. Tao, C. Kong, L. Chen, High performance ZIF-8 molecular sieve membrane on hollow ceramic fiber via crystallizing-rubbing seed deposition, *Chem. Eng. J.* 220 (2013) 1–5, <https://doi.org/10.1016/j.cej.2013.01.051>.
- [61] T. Tomita, K. Nakayama, H. Sakai, Gas separation characteristics of DDR type zeolite membrane, *Microporous Mesoporous Mater.* 68 (2004) 71–75, <https://doi.org/10.1016/j.micromeso.2003.11.016>.
- [62] S.R. Venna, M.A. Carreon, Highly permeable zeolite imidazolate framework-8 membranes for CO<sub>2</sub>/CH<sub>4</sub> separation, *J. Am. Chem. Soc.* 132 (2010) 76–78, <https://doi.org/10.1021/ja909263x>.
- [63] L.S. Lai, Y.F. Yeong, K. Keong Lau, M.S. Azmi, Zeolitic imidazolate frameworks (ZIF): a potential membrane for CO<sub>2</sub>/CH<sub>4</sub> separation, *Sep. Sci. Technol.* 49 (2014) 1490–1508, <https://doi.org/10.1080/01496395.2014.903281>.

- [64] M. Shah, H.T. Kwon, V. Tran, S. Sachdeva, H.K. Jeong, One step *in situ* synthesis of supported zeolitic imidazolate framework ZIF-8 membranes: role of sodium formate, *Microporous Mesoporous Mater.* 165 (2013) 63–69, <https://doi.org/10.1016/j.micromeso.2012.07.046>.
- [65] R. Das, D. Mehta, H. Bhardawaj, An overview on microwave mediated synthesis, *Int. J. Res. Dev. Pharm. Life Sci.* 1 (2012) 32–39.
- [66] H.T. Kwon, H.-K. Jeong, Highly propylene-selective supported zeolite-imidazolate framework (ZIF-8) membranes synthesized by rapid microwave-assisted seeding and secondary growth, *Chem. Commun.* 49 (2013) 3854, <https://doi.org/10.1039/c3cc41039k>.
- [67] F. Hillman, J.M. Zimmerman, S.-M. Paek, M.R.A. Hamid, W.T. Lim, H.-K. Jeong, Rapid microwave-assisted synthesis of hybrid zeolitic-imidazolate frameworks with mixed metals and mixed linkers, *J. Mater. Chem. A* 5 (2017) 6090–6099, <https://doi.org/10.1039/C6TA11170J>.
- [68] X. Li, Y. Liu, J. Wang, J. Gascon, J. Li, B. Van Der Bruggen, Metal-organic frameworks based membranes for liquid separation, *Chem. Soc. Rev.* 46 (2017) 7124–7144, <https://doi.org/10.1039/c7cs00575j>.
- [69] X. Liu, Y. Li, G. Zhu, Y. Ban, L. Xu, W. Yang, An organophilic pervaporation membrane derived from metal-organic framework nanoparticles for efficient recovery of bio-alcohols, *Angew. Chem. Int. Ed. Engl.* 50 (2011) 10636–10639, <https://doi.org/10.1002/anie.201104383>.
- [70] H. Ruan, C. Guo, H. Yu, C. Gao, A. Sotito, B. Van Der Bruggen, Fabrication of a MIL-53 (Al) nanocomposite membrane and potential application in desalination of dye solutions, *Ind. Eng. Chem. Res.* 53 (2016) 1–32, <https://doi.org/10.1021/acs.iecr.6b03201>.
- [71] B. Yao, W. Jiang, Y. Dong, Z. Liu, Y. Dong, Post-synthetic polymerization of UiO-66-NH<sub>2</sub> nanoparticles and polyurethane oligomer toward stand-alone membranes for dye removal and separation, *Chem. Eur. J.* 22 (2016) 10565–10571, <https://doi.org/10.1002/chem.201600817>.
- [72] H.T. Kwon, H.-K. Jeong, *In situ* synthesis of thin zeolitic-imidazolate framework ZIF-8 membranes exhibiting exceptionally high propylene/propane separation, *J. Am. Chem. Soc.* 135 (2013) 10763–10768, <https://doi.org/10.1021/ja403849c>.
- [73] E. Jang, E. Kim, H. Kim, T. Lee, H.J. Yeom, Y. W. Kim, J. Choi, Formation of ZIF-8 membranes inside porous supports for improving both their H<sub>2</sub>/CO<sub>2</sub> separation performance and thermal/mechanical stability, *J. Membr. Sci.* 540 (2017) 430–439, <https://doi.org/10.1016/j.memsci.2017.06.072>.
- [74] L. Li, J. Yao, R. Chen, L. He, K. Wang, H. Wang, Infiltration of precursors into a porous alumina support for ZIF-8 membrane synthesis, *Microporous Mesoporous Mater.* 168 (2013) 15–18, <https://doi.org/10.1016/j.micromeso.2012.09.029>.
- [75] Y. Ying, D. Liu, W. Zhang, H. Huang, Q. Yang, C. Zhong, High-flux graphene oxide membranes intercalated by MOF with highly selective separation of aqueous organic solution, *Appl. Mater. Interfaces* (2016) <https://doi.org/10.1021/acsami.6b14371>.
- [76] J.W. Maina, J. Schutz, L. Grundy, E. Des Ligneris, L. Kong, C. Pozo-gonzalo, M. Ionescu, L. F. Dumée, Inorganic nanoparticles/metal organic framework hybrid membrane reactors for efficient photocatalytic conversion of CO<sub>2</sub>, *ACS Appl. Mater. Interfaces* 9 (2017) 35010–35017, <https://doi.org/10.1021/acsami.7b11150>.
- [77] S. Sorribas, A. Kudasheva, E. Almendro, B. Zornoza, Ó. De, C. Téllez, J. Coronas, Pervaporation and membrane reactor performance of polyimide based mixed matrix membranes containing MOF HKUST-1, *Chem. Eng. Sci.* 124 (2015) 37–44, <https://doi.org/10.1016/j.ces.2014.07.046>.
- [78] X. Dong, Y.S. Lin, Synthesis of an organophilic ZIF-71 membrane for pervaporation solvent separation, *Chem. Commun.* 49 (2013) 1196–1198, <https://doi.org/10.1039/c2cc38512k>.
- [79] S. Wang, Z. Kang, B. Xu, L. Fan, G. Li, L. Wen, X. Xin, Z. Xiao, J. Pang, X. Du, D. Sun, Wettability switchable metal-organic framework membranes for pervaporation of water/ethanol mixtures, *Inorg. Chem. Commun.* 82 (2017) 64–67, <https://doi.org/10.1016/j.inoche.2017.05.016>.
- [80] X. Liu, H. Jin, Y. Li, H. Bux, Z. Hu, Y. Ban, W. Yang, Metal-organic framework ZIF-8 nanocomposite membrane for efficient recovery of furfural via pervaporation and vapor permeation, *J. Membr. Sci.* 428 (2013) 498–506, <https://doi.org/10.1016/j.memsci.2012.10.028>.
- [81] X. Liu, C. Wang, B. Wang, K. Li, Novel organic-dehydration membranes prepared from zirconium metal-organic frameworks, *Adv. Funct. Mater.* 27 (2017) 1–6, <https://doi.org/10.1002/adfm.201604311> 1604311.

- [82] W. Xiaocao, W. Wan, J. Jianwen, C. Jurgen, H. Aisheng, High-flux high-selectivity metal-organic framework MIL-160 membrane for xylene isomer separation by pervaporation, *Angew. Chem. Int. Ed. Engl.* (2018) <https://doi.org/10.1002/anie.201807935>.
- [83] S. Basu, M. Maes, A. Cano-Odena, L. Alaerts, D.E. De Vos, I.F.J. Vankelecom, Solvent resistant nanofiltration (SRNF) membranes based on metal-organic frameworks, *J. Membr. Sci.* 344 (2009) 190–198, <https://doi.org/10.1016/j.memsci.2009.07.051>.
- [84] S. Sorribas, P. Gorgojo, C. Tellez, J. Coronas, A.G. Livingston, High flux thin film nanocomposite membranes based on MOFs for organic solvent nanofiltration, *J. Am. Chem. Soc.* 135 (2013) 15201–15208, <https://doi.org/10.1021/ja407665w>.
- [85] J. Campbell, J.D.S. Bursal, G. Szekely, R.P. Davies, D.C. Braddock, A. Livingston, Hybrid polymer/MOF membranes for organic solvent nanofiltration (OSN): chemical modification and the quest for perfection, *J. Membr. Sci.* 503 (2016) 166–176, <https://doi.org/10.1016/j.memsci.2016.01.024>.
- [86] X. Guo, D. Liu, T. Han, H. Huang, Q. Yang, C. Zhing, Preparation of thin film nanocomposite membranes with surface modified MOF for high flux organic solvent nanofiltration, *AIChE J.* 63 (2016) 1301–1312, <https://doi.org/10.1002/aic>.
- [87] H. Yang, N. Wang, L. Wang, H.X. Liu, Q.F. An, S. Ji, Vacuum-assisted assembly of ZIF-8@GO composite membranes on ceramic tube with enhanced organic solvent nanofiltration performance, *J. Membr. Sci.* 545 (2018) 158–166, <https://doi.org/10.1016/j.memsci.2017.09.074>.
- [88] L. Wang, M. Fang, J. Liu, J. He, J. Li, J. Lei, Layer-by-layer fabrication of high-performance polyamide/ZIF-8 nanocomposite membrane for nanofiltration applications, *ACS Appl. Mater. Interfaces* 7 (2015) 24082–24093, <https://doi.org/10.1021/acsami.5b07128>.
- [89] Z. Junyong, Q. Lijuan, U. Andrew, J. Hou, W. Jing, Z. Yatao, L. Xin, Y. Shushan, L. Jian, T. Miaomiao, L. Jiuyang, B. Van Der Bruggen, Elevated performance of thin film nanocomposite membranes enabled by modified hydrophilic MOFs for nanofiltration, *ACS Appl. Mater. Interfaces* (2016) <https://doi.org/10.1021/acsami.6b14412>.
- [90] S. Basu, M. Balakrishnan, Polyamide thin film composite membranes containing ZIF-8 for the separation of pharmaceutical compounds from aqueous streams, *Sep. Purif. Technol.* 179 (2017) 118–125, <https://doi.org/10.1016/j.seppur.2017.01.061>.
- [91] Z. Rao, K. Feng, B. Tang, P. Wu, Surface decoration of amino-functionalized metal-organic framework/graphene oxide composite onto polydopamine coated membrane substrate for highly efficient heavy metal removal, *Appl. Mater. Interfaces* (2016) 1–39, <https://doi.org/10.1021/acsami.6b15873>.
- [92] J. Duan, Y. Pan, F. Pacheco, E. Litwiller, Z. Lai, I. Pinnau, High-performance polyamide thin-film nanocomposite reverse osmosis membranes containing hydrophobic zeolitic imidazolate framework-8, *J. Membr. Sci.* 476 (2015) 303–310, <https://doi.org/10.1016/j.memsci.2014.11.038>.
- [93] K. Sumida, D.L. Rogow, J.A. Mason, T.M. McDonald, E.D. Bloch, Z.R. Herm, T. Bae, J.R. Long, Carbon dioxide capture in metal-organic frameworks, *Chem. Rev.* 112 (2012) 724–781, <https://doi.org/10.1021/cr2003272>.
- [94] R. Zabao, J.B. James, A. Kasik, Y.S. Lin, Metal-organic framework membrane process for high purity CO<sub>2</sub> production, *AIChE J.* (2016) 1–6, <https://doi.org/10.1002/aic>.
- [95] K. Aylin, L.H. Wee, P. Martin, B. Sara, A.M. Johan, V. Ivo, F.J., highly selective gas separation membrane using *in situ* amorphised metal-organic frameworks, *Energy Environ. Sci.* 10 (2017) 2342, <https://doi.org/10.1039/c7ee01872j>.
- [96] O. Shekhah, V. Chernikova, Y. Belmabkhout, M. Eddaoudi, Metal-organic framework membranes: from fabrication to gas separation, *Crystals* 8 (2018) 412, <https://doi.org/10.3390/cryst8110412>.
- [97] T.M. Nenoff, MOF membranes put to the test, *Nat. Publ. Group* 7 (2015) 377–378, <https://doi.org/10.1038/nchem.2218>.
- [98] Y. Liu, Z. Ng, E.A. Khan, H. Jeong, C. Ching, Z. Lai, Microporous and mesoporous materials synthesis of continuous MOF-5 membranes on porous  $\alpha$ -alumina substrates, *Microporous Mesoporous Mater.* 118 (2009) 296–301, <https://doi.org/10.1016/j.micromeso.2008.08.054>.
- [99] H. Guo, G. Zhu, I.J. Hewitt, S. Qiu, “Twin Copper Source” growth of metal-organic framework membrane: Cu<sub>3</sub>(BTC)<sub>2</sub> with high permeability and selectivity for recycling H<sub>2</sub>, *J. Am. Chem. Soc.* 131 (2009) 1646–1647.

- [100] H. Bux, F. Liang, Y. Li, J. Cravillon, M. Wiebcke, Zeolitic imidazolate framework membrane with molecular sieving properties by microwave-assisted solvothermal synthesis, *J. Am. Chem. Soc.* 131 (2009) 16000–16001, <https://doi.org/10.1021/cm902032y>.

### Further reading

- [101] Y. Zhao, Z. Song, X. Li, Q. Sun, N. Cheng, S. Lawes, Metal organic frameworks for energy storage and conversion, *Energy Storage Mater.* 2 (2016) 35–62, <https://doi.org/10.1016/j.ensm.2015.11.005>.
- [102] J. Wang, Y. Wang, Y. Zhang, A. Uliana, J. Zhu, J. Liu, B. Van Der Bruggen, Zeolitic Imidazolate framework/graphene oxide hybrid nanosheets functionalized thin film nanocomposite membrane for enhanced antimicrobial performance, *ACS Appl. Mater. Interfaces* 8 (2016) 25508–25519, <https://doi.org/10.1021/acsami.6b06992>.